# TRANSIENT WELLBORE PRESSURIZATION CORRELATION & HIPPS RESPONSE TIME IN MULTIPHASE FLOW

BY


**AHMED A. HOMOUD**


A Thesis Presented to the
DEANSHIP OF GRADUATE STUDIES

**KING FAHD UNIVERSITY OF PETROLEUM & MINERALS**

DHAHRAN, SAUDI ARABIA

In Partial Fulfillment of the
Requirements for the Degree of

# MASTER OF SCIENCE

**In**

PETROLEUM ENGINEERING

**May 2018**

KING FAHD UNIVERSITY OF PETROLEUM & MINERALS

DHAHRAN- 31261, SAUDI ARABIA

**DEANSHIP OF GRADUATE STUDIES**

This thesis, written by **Ahmed A. Homoud** under the direction his thesis advisor and approved by his thesis committee, has been presented and accepted by the Dean of Graduate Studies, in partial fulfillment of the requirements for the degree of **MASTER OF SCIENCE IN PETROLEUM ENGINEERING.**

Dr. Rahul N. Gajbhiye
(Advisor)

Dr. Dhafer A. Al Shehri
Department Chairman

Dr. Dhafer A. Al Shehri
(Co-Advisor)

Dr. Salam A. Zummo
Dean of Graduate Studies

Dr. Bashirul Haq
(Member)

10\5\18

Date

Salaheldin Elkatatny

Dr. Salaheldin M. Elkatatny
(Member)

Dr. Mohamed Mahmoud
(Member)

The work presented in this thesis is dedicated to my parents who raised me and taught me to respect science. To my beloved wife who encouraged and supported me throughout my study. To my newly born child, my hope in life.

# ACKNOWLEDGMENTS

I would like to acknowledge my advisor Dr. Rahul Gajbhiye for his continuous support and guidance throughout my thesis work. His comments and feedbacks provided a second point of view for solving complex situations. I also would like to acknowledge my co-advisor and committee members for their dedication to review my work. A special thanks to my coworker at Saudi Aramco Dr. Mikal Espedal who provided all necessary support to make this work possible. Finally, I would like to acknowledge my fellow students Ala Al-Dogail and Zeeshan Tariq for their endless support.

# TABLE OF CONTENTS

# LIST OF TABLES

# LIST OF FIGURES

# LIST OF ABBREVIATIONS

**1OO2:** One out of Two Voting System.

**2OO3:** Two out of Three Voting System.

**a, b, and c**: Constants for Pressure Build-up Quadratic Equation.

**A:** Non-Linear Regression Constant= 2.316.

**B:** Non-Linear Regression Constant= 0.012.

**bpd:** Barrels Per Day.

**C:** Non-Linear Regression Constant= -0.738.

**D:** Non-Linear Regression Constant= 0.067.

**E:** Non-Linear Regression Constant= -14.397.

**EOS:** Equation of State

**ESD:** Emergency Shut Down.

**F:** Non-Linear Regression Constant= 0.531.

**ft:** Feet

**FWHP:** Flowing Wellhead Pressure.

**G:** Non-Linear Regression Constant= 3.426.

**GOR:** Gas Oil Ratio

**H:** Non-Linear Regression Constant= 0.024.

**HIPPS:** High Integrity Pressure Protection System

**I:** Non-Linear Regression Constant= -2.286E-42.

**ID:** Inner Diameter.

**in:** Inch.

**J:** Non-Linear Regression Constant= 9.900.

**K:** Non-Linear Regression Constant= -4.972.

**L:** Non-Linear Regression Constant= 0.065.

**M:** Non-Linear Regression Constant= 1.313.

**MD:** Measured Depth.

**MW:** Molecular Wight.

**N:** Non-Linear Regression Constant= -280.276.

**O:** Non-Linear Regression Constant= 0.036.

**P:** Non-Linear Regression Constant= -3472.949.

**Pb:** Bubble Point Pressure.

**PFD:** Probability of Failure.

**PI:** Productivity Index, barrel per day per psi.

**PLV:** Pad Limit Valve.

**Pmax:** Maximum Pressure Reached During the Transient Pressurization Period.

**PST:** Process Safety Time.

**Q:** Non-Linear Regression Constant= 0.001.

**R:** Non-Linear Regression Constant= 3794.112.

**SIL:** Safety Integrity Level.

**SIS:** Safety Instrumented System.

**SIWHP:** Shut-in Wellhead Pressures.

$\boldsymbol{T(P_{Max})}$**:** Time to Reach PMax.

**TVD:** True Vertical Depth.

# ABSTRACT

Full Name : Ahmed Abdulkarim Abdullah Homoud

Thesis Title : Transient Wellbore Pressurization Correlation & HIPPS Response Time in Multiphase Flow

Major Field : M.SC. Degree in Petroleum Engineering

Date of Degree : May 2018

HIPPS (High Integrity Pressure Protection System) is a widely used system in the petroleum industry to protect downstream flowlines that are rated below the full SIWHP (Shut-in Wellhead Pressure) from high-pressure events. The development of wells with high shut-in pressures makes it increasingly expensive to design the flowlines with a conventional mechanical form of protection. Therefore, selecting a thinner flowline wall and reduced pressure class flanges valves and other equipment could reduce material and overall CAPEX costs and favored as the economic option. In the absence of mechanical protection and relief systems in these underrated flowlines, HIPPS becomes the primary pressure protection method, if traditional Emergency Shut-Down (ESD) system protection should fail.

According to the Minerals Management Service and Granherne Limited, there is a significant risk involved in high pressure and high rate wells. Therefore, HIPPS implementation requires a better understanding of the implications of timing, testing, and material selection in order to justify regulatory requirements. One of the key requirements is determining the “High-High” trip point, the minimum setting pressure required for activating the system. This calculation is crucial to the performance of the system since it

is defined by the envelope of the wellbore pressure build-up time. Another key requirement to determine the High-High trip point is HIPPS Valve Response Time, which varies based on valves type and vendor providers.

In this transient flow assurance study, the aim is to develop a generalized correlation to estimate the wellbore pressure build-up time for the selected fields taking into account different studied parameters. The study covers data from three oil fields with various Fluid Properties, GOR's, Reservoir Pressures, Productivity Index, Depths and Shut-in Wellhead Pressures (SIWHPs). The study will investigate the effect of each parameter on the pressure build-up time and relate it to the system trip point. Then, the optimum "High-High" trip points for each field will be defined based on analysis of the pressure build-up effects to the downstream flowline at the worst-case.

The worst-case is defined as a blockage that may occur to the downstream flowlines near the HIPPS system. It varies based on the specifics of the system being investigated. For instance, the downstream valve/blockage may be a valve or it may be a hydrate plug that has formed somewhere in the flowline. In this study, the blockage is defined as a sudden shutdown of the Pad Limit Valve (PLV).

# ملخص الرسالة

**الاسم الكامل**: أحمد عبدالكريم عبدالله حمود

**عنوان الرسالة:** علاقة لحساب ضغط آبار النفط الأولية واستجابة نظام الحماية من الضغط العالي.

**التخصص:** ماجستير في هندسة البترول

**تاريخ الدرجة العلمية**: مايو 2018


نظام الحماية من الضغط العالي هو نظام يستخدم على نطاق واسع في الصناعة البترولية لحماية خطوط تدفق النفط الخام والتي يتم تصنيفها أقل من ضغط البئر المقفلة كليًا. إن تطوير الآبار ذات ضغط إغلاق عالٍ يجعل تصميم خطوط التدفق مع حماية ميكانيكية تقليدية مكلف بشكل متزايد. لذلك ، فإن اختيار سمك جدار أقل لأنابيب التدفق وغيرها من المعدات يمكن أن يقلل من تكاليف المواد والتكاليف الشاملة ويفضل كخيار اقتصادي. وفي غياب أنظمة الحماية الميكانيكية التقليدية في خطوط التدفق هذه ، يصبح نظام الحماية من الضغط العالي هو طريقة الحماية الأساسية في حالة الضغط العالي.

وفقا لإدارة خدمات المعادن وشركة Granherne المحدودة ، هناك خطر كبير ينطوي بتطوير آبار الضغط والإنتاج العالية. لذلك ، يتطلب تطبيق نظام الحماية من الضغط العالي فهمًا أفضل لآثار التوقيت واختيار المواد من أجل تبرير متطلبات التنفيذ. يتمثل أحد المتطلبات الأساسية في تحديد نقطة الاستجابة "عالية-عالية" ، وهي الحد الأدنى للضغط اللازمة لتنشيط النظام. يعتبر حساب هذه النقطة حاسمًا لأداء النظام نظرًا لأنه يتم تحديده من خلال وقت تراكم ضغط البئر. ومن المتطلبات الرئيسية الأخرى لتحديد نقطة الاستجابة هي وقت استجابة صمام النظام ، والذي يختلف بناءً على نوع الصمامات وشركات توفير النظام.

في هذه الدراسة لضمان التدفق العابر، فإن الهدف هو تطوير علاقة لتقدير وقت تراكم ضغط البئر للحقول المختارة ، مع الأخذ بعين الاعتبار البيانات المتوفرة. تغطي الدراسة بيانات من ثلاثة حقول نفطية مع خصائص مختلفة من سوائل

، نسبة الغاز من الزيت ، ضغوط المكمن ، مؤشرات الإنتاجية ، العمق و ضغوط البئر المقفلة كليًا. سوف تقوم الدراسة بالتحقق من تأثير كل خاصية على وقت تراكم الضغط وربطه بنقطة استجابة نظام الحماية من الضغط العالي. بعد ذلك ، سيتم تحديد نقاط الاستجابة "عالية-عالية" المثلى لكل حقل بناءً على تحليل تأثيرات تراكم الضغط في البئر في أسوأ الحالات.

يتم تعريف أسوأ الحالات على أنها انسداد قد يحدث لخطوط التدفق بالقرب من نظام الحماية من الضغط العالي. تختلف تلك الحالة بناءً على تفاصيل النظام الجاري التحقيق فيه. على سبيل المثال ، قد يكون الانسداد هو اغلاق مفاجئ للصمام أو قد يكون سدادة هيدرات تكونت في مكان ما في خط التدفق. في هذه الدراسة ، يتم تعريف الانسداد على أنه إغلاق مفاجئ للصمام.

# CHAPTER 1

# INTRODUCTION

HIPPS (High Integrity Pressure Protection System) is a widely used system in the petroleum industry to protect downstream flowlines that are rated below the full SIWHP (Shut-in Wellhead Pressure) from high-pressure events.

According to the Minerals Management Service and Granherne Limited, there is a significant risk involved in high pressure and high rate wells. Therefore, HIPPS implementation requires a better understanding of the implications of timing, testing, and material selection in order to justify regulatory requirements.

In this transient flow assurance study, the aim is to develop a generalized correlation to estimate the wellbore pressure build-up time for the selected fields taking into account different studied parameters. The study covers data from three oil fields with various Fluid Properties, GOR's, Reservoir Pressures, Productivity Index, Depths and Shut-in Wellhead Pressures (SIWHPs). The study will investigate the effect of each parameter on the pressure build-up time.

The modeling part objective is to predict wellhead pressure build-up time and behavior at the shut-in condition for 21 wells. The models include well model, surface piping until Pad Limit Valve (PLV) and PVT data. The well models were calibrated against field measurements to match the actual reservoir pressure, productivity index (PI), flowing wellhead pressure (FWHP), shut-in wellhead pressure (SIWHP) and flow rates.

The results from the transient hydraulic simulation model are then presented. Sensitivity to input parameters were highlighted to determine the most influential parameters to the results. Lastly, an empirical correlation to predict pressure at an early shut-in time is introduced.

# CHAPTER 2

# LITERATURE REVIEW

## 2.1 HIPPS OVERVIEW

HIPPS are Safety Instrumented Systems (SIS) aim to isolate downstream pipelines from high-pressure conditions developing at the facilities and flowlines. The source of the high-pressure events can be either from upstream and/or downstream of the well for example; process trip, hydrate formation, inadvertent valves closure, loss of control of a well, or any other blockage. In the incident of an overpressure, the HIPPS shall isolate the flowlines from the high- pressure source. Hence, downstream pipelines could be rated below the full shut-in pressure (SIP) of the upstream well, which corresponds to lower material and overall CAPEX costs. Furthermore, HIPPS can also allow for reducing the downstream equipment rating like separators, risers and process plant, and can favor economics of field developments as a viable option by utilizing existing infrastructure that has lower pressure rating equipment.

In general, HIPPS consists of pressure sensors, controllers, and valves. HIPPS shall have a very high level of reliability, which is explained as a Safety Integrity Level (SIL), or probability of failure (PFD). There are four SIL levels which usually varies from SIL1 to SIL4, SIL4 has the lowest PFD. HIPPS are required to achieve SIL3 as per international standards (Curran, 2008). This high-level requirement will typically necessitate high integrity and high HIPPS availability joined with redundancy, autonomous shutdown functions, remote communications, and regular testing and monitoring.

The HIPPS components are presented in the below Figure 1 and are as following:

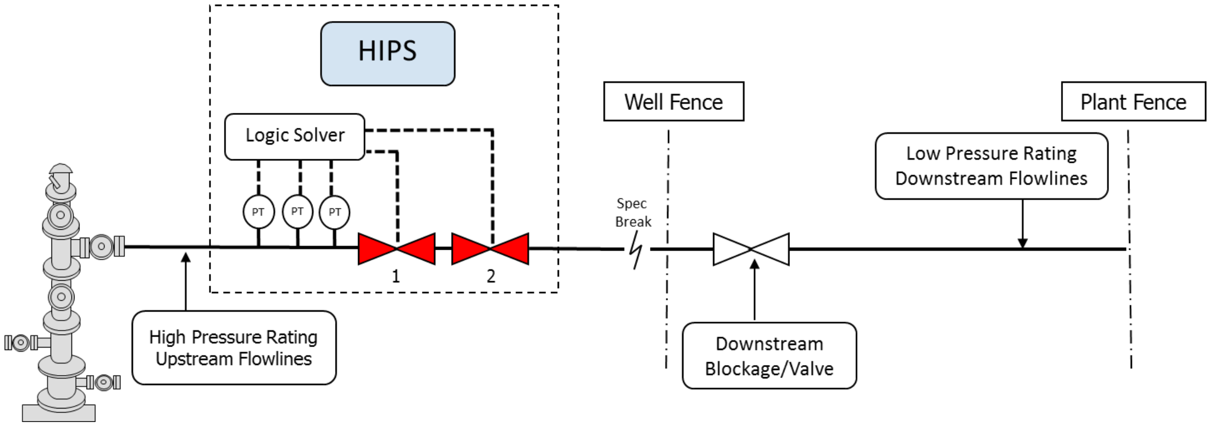


**Figure 1 HIPPS System Components**

1. Pressure Transducers

Figure 1 shows three pressure sensors placed between the HIPPS valves. The number of sensors and their logic system is a function of required reliability and probability of failure. The system presented in the figure is categorized as dual 2oo3 voting where sensing of the high-pressure event by two transducers in either bank would activate the HIPPS.

2. HIPPS Controller (Logic Solver)

HIPPS requires an independent controller, which manages the pressure sensors. The controller closes the HIPS valves if an overpressure scenario is detected. Operational testing is also being conducted by using a controller.

3. HIPPS Valves

HIPPS valves are the last component, which segregates the system from the overpressure risk. Figure 1 shows two HIPPS valves, which is typical of Safety Integrity Level (SIL) 3 rating. An extra HIPPS test valve is also required to allow for operational testing.

## 2.2 HIPPS MAIN FUNCTIONS

Historically, flowlines have been rated to handle the full wellhead shut-in pressure (SIWHP), which will eventually have a significant cost of the field development. Especially if the flowlines are long and therefore will require a significant amount of steel to build.

The cost of the flowlines can be reduced by lowering its wall thickness and hence its pressure rating; the thinner the wall thickness the lower the cost. Therefore, downstream flowlines could be rated below the full shut-in pressure (SIP) of the upstream well, which corresponds to lower material and overall CAPEX costs. Furthermore, HIPPS can also allow for reducing the downstream equipment rating like separators, risers and process plant, and can favor economics of field developments as a viable option by utilizing existing infrastructure that has lower pressure rating equipment.

In extreme cases and specifically in offshore deep reservoirs, subsea HIPPS can become essential to install in order to develop the field. This is because of the fact that pipelines would be too heavy to be lifted and transported offshore using the currently available technology. It worth mentioning that at least one oil operator company worldwide would only consider using HIPPS where there is no other technical solution, favoring not to utilize it as a cost-reduction alternative where it is possible to use a full rated SIWHP flowline (Hutching, 2010).

Benefits of using HIPPS:

- Reduce flowline wall thickness.
- Reduce welding time, specifically in offshore.
- Potential to use existing lower pressure rating flowlines.

Disadvantages of using HIPPS:

- Complication to the flowlines system and seen as a source of unreliability.
- Difficulties in HIPPS valves testing.
- A Potential of hydrates formation.

## 2.3 HIPPS DEVELOPMENT HISTORY

As per (Hutching, 2014), there are 11 installed subsea HIPPS until 2010 with all but two located in the North Sea. Table 1 shows these projects with the operators, installation dates and other details. Amongst the projects listed, there are examples of no damage, no burst and burst critical systems.

This modest total illustrates the relatively slow adoption of sub-sea pressure protection systems, although there appears to be a much-increased interest within the industry in more recent times. General Electric (GE) is also aware of a number of potential new HIPPS projects some on a large scale.

The first ever HIPPS, which was the Shell's Kingfisher project, was installed in 1997 with the most recent of the 11 projects installed in 2008. There are also 3 other projects currently in execution, giving a grand total of just 14 projects of which 4 systems are attributable to GE Oil and Gas/VetcoGray products.

Including GE, there are now five subsea equipment suppliers able to offer HIPPS to their customers, and to date, nine oil companies have invested in at least one subsea pressure protection system. It is also noted that despite the original subsea HIPPS being installed some 13 years ago, two of the equipment supplier companies listed have less than three years installed experience.

**Table 1 Subsea HIPPS Development History**

| **Operator** | **Project** | **Date** | **Pressure (psi)** | **Supplier** |
|---|---|---|---|---|
| **Shell** | Kingfisher | 1997 | 10,000 | Aker Solutions |
| **Statoil** | Gulfaks | 2000 | 10,000 | FKS |
| **Shell** | Scoter | 2002 | 1,300 | Aker Solutions |
| **Shell** | Penguins | 2002 | 8,250 | Aker Solutions |
| **BG** | Juno | 2002 | 5,000 | Aker Solutions |
| **BP** | Rhum | 2005 | 10,300 | VetcoGray |
| **Statoil** | Kristin | 2005 | 10,700 | Aker Solutions |
| **Talisman** | Tweedsmuir | 2006 | 6,000 | VetcoGray |
| **Total** | Jura | 2008 | 10,000 | Dril-Quip |
| **Nexus** | Longtom | 2008 | - | Cameron |
| **Petrobras** | Mexilhao | 2008 | 10,000 | FKS |
| **BP** | Block31 | Aw 2009 | - | Cameron |
| **BP** | Devenick | Aw 2009 | 8,450 | VetcoGray |
| **ENI** | Denise B | Aw 2009 | 3,450 | VetcoGray |

## 2.4 HIPPS INTERNATIONAL STANDARDS

There are four international standards available to assist with the design, testing, operating and documentation required to implement HIPPS: Full form IEC 6158 (2000), IEC 61511 (2003), OLF 070 (2004) and API 17O (2009).

The IEC 61508 and IEC 61511 are international standards that provide requirements for safety instrumented system (SIS) design, specification, installation, maintenance, and operation so that it can be surely trusted to maintain the safety of the process.

The IEC 61511 is an application of IEC 61508 for process sector. Manufacturers and suppliers of devices usually trail the IEC 61508, whereas integrators, system designers and operators usually trail IEC 61511. This means that a manufacturer of HIPPS hardware devices (e.g. sensors, logic solvers or valves) should use IEC 61508 to verify and validate compliance with functional safety requirements. The only exception to this rule is if the manufacturer or supplier claims compliance with functional safety requirements based on a 'proven in use' argument. In this case, IEC 61511 should be followed as it provides requirements for claiming 'proven in use' for components that have not been fully validated according to IEC 61508.

OLF 070 is a Norwegian petroleum industry standard. The overall objective of the OLF 070 is to deliver a guide on the applications of IEC 61508 and IEC 61511 and thus simplify their use in the petroleum industry. The guidelines provide practical help for the functional safety system designer, including identifying the minimum SIL requirements for standard functions. OLF The API 17-O standard is the only document specifically aimed at HIPPS. It was not issued until October 2009 and updated in July 2014 (although it was in draft form for some time). Initially, concern was expressed that because of its rather late arrival, the new recommended practice might conflict with the earlier standards and indeed potentially be at odds with currently installed designs. Fortunately, this does not appear to be the case as API 17-O refers to the IEC 6158 and IEC 61511 generic standards in several places and directly extracts relevant tables from them. Further, as described earlier OLF 070 contains relatively few references to HIPPS but once again there does not appear to be any direct conflict with the API 17-O recommended practice. Because the new recommended practice is dedicated to HIPPS, it gives guidance on the elements that must be considered for design, testing, quality control, verification and validation, installation and commissioning of these systems and, as such, must be considered a useful tool.

## 2.5 DOWNSTREAM FLOWLINE DESIGN

There are three different criticality methods at which the flowline wall thickness can be lowered: no-damage, no-burst and burst critical. The 'no-damage' is when the flowline yield and burst pressures both surpass the well shut-in pressure. The 'no-burst' is when the yield pressure is less than the well shut-in pressure, however, the burst pressure will still surpass the shut-in pressure. The 'burst critical' is when the flowline yield and burst pressures are both less than the well shut-in pressure. Note that as the cost savings increased, the risk would increase due to selecting lower criticality level, as illustrated in Figure 3 (Hutchings, 2010).

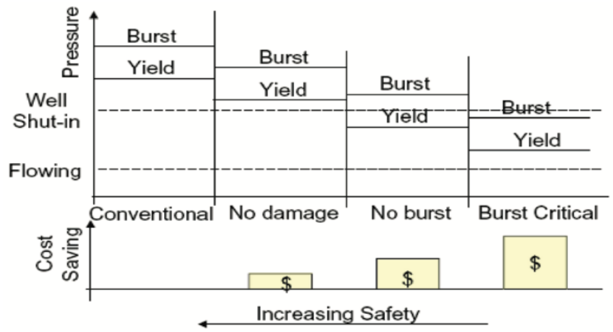


**Figure 2 Different Levels of HIPPS Criticality**

As per API Standard 17O, the possibility of abrupt blockage of the flowline at various points downstream of the HIPPS shall be considered. Calculations of the transient pressure increase arising from the blockages should be developed. Transient pressure calculations provide key guidance to designers on the minimum shut-in time necessary for the HIPPS to avoid overpressure of the flowline between the blockage and the HIPPS. It is essential that personnel with experience and knowledge scrutinize and validate transient pressure calculations.

To accomplish this, the sum of the logic solver reaction period and the response time to attain a safe state should be less than the PST "Process Safety Time". In case of a high-pressure event, the available time until a hazardous incident takes place is called the PST.

## 2.6 Fortified Zone – Directly Downstream of HIPPS

If the HIPPS fails to shut down during overpressure scenario, the pipeline will continue to pressurize up until it will ultimately reach a pressure at which it bursts. To make sure that the flowline does not burst directly downstream of the HIPPS location a section of fortified can be incorporated (Curran,2008). The reasons that drive this are as following:

1. To make sure that the downstream flowline will not rupture close to the Christmas tree or the manifold at which manned operations could be ongoing.

2. In case of hydrate formation in the downstream flowline, it could cause a faster pressure buildup than the HIPPS could react to.

Hydraulic simulations shall be conducted to define the optimum balance between pressure build-up time and HIPPS valve closure speed. The probability of hydrate forming immediately downstream of the HIPPS could be argued as very unlikely during normal steady-state operations. However, this event could be more critical during transient flow, i.e. start-up conditions with methanol injection. Therefore, each project must be evaluated to determine under what circumstances a blockage could occur immediately downstream the HIPPS.

## 2.7 HIPPS Safety Integrity Level

As a measure of the availability and quality of a safety function system, the term safety integrity level (SIL) was presented in the international standards; IEC-61508/61511 and it has been used internationally, particularly in Europe and United Kingdom.

Safety Integrity Level assesses the level of a Safety Instrumented System quantitatively so that to verify whether the target degree of safety is achieved or not. It assists to safeguard the safety of the flowlines and facilities by improving the SIS in order to reach the target integrity level. It is a way to evaluate the level of probability whether to fulfill the designated SIS's of the safety-instrumented function (SIF). As in Table 2, SIL has a range of values as captured from the IEC standard which varies from level 1 to 4.

**Table 2 SIL According to IEC Standard versus Safety Availability**

| IEC 61508-SIL | Safety Instrumented System Performance Requirement | |
|---|---|---|
| | **Safety Availability Requirement, %** | **Average Probability of Failure, $PFD_{avg}$** |
| 1 | 90.00 – 99.00 | $10^{-1} – 10^{-2}$ |
| 2 | 99.00 – 99.90 | $10^{-2} – 10^{-3}$ |
| 3 | 99.90 – 99.99 | $10^{-3} – 10^{-4}$ |
| 4 | >99.99 | $<10^{-4}$ |

The common industrial SIL for HIPPS is SIL 3 which is equivalent to $10^{-3} – 10^{-4}$ PFD, as provided in IEC 61508. Inbok Lee and Taekeun Oh conducted a study to examine the change of a SIL by changing the number of pressure transducers and HIPPS valves, which is, the number of instruments. The change of a SIL by changing the test frequency and interval (inspection interval) was also examined for the improvement in the availability and reliability of a system. Finally, taking into account the instrument reliability and redundancy, SIL variations were studied.

One of the easy ways to improve the safety integrity level (SIL) is to increase the availability and reliability of a system simply by connecting additional instruments. Figure 3 demonstrates an example showing the increase of instrument's number. The 2oo3 shows that the two out of three sensors are receiving orders by the voting system and 1oo2 final element is to increase availability and reliability.

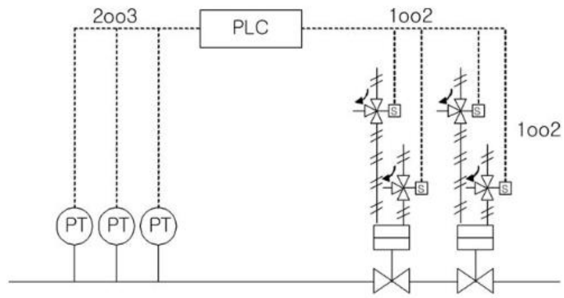


**Figure 3 Schematic Drawings of 2OO3-1OO2 Voting System**

Table 3 summarizes the outcomes of the three cases, with maintaining the testing period to be once every three years assuming that the facilities have been operated without shutdown for three consecutive years. The results show that as the number of sensors increases, hence increasing redundancy to a final element, it can lead up to SIL 2 system. In addition, by the adding additional sensors the SIL increases, however, the system does not reach the SIL 3 level which is a requirement for HIPPS by just adding an extra number of instruments.

The differences in SIL was then also calculated by changing the test period. The change in SIL was estimated by altering the test period from once every six months, three months, and two months, separately. Table 4 summarizes the results. It was confirmed that it is possible to attain SIL-3 by increasing the regularity of a testing utilizing the same instrument as of Case 3.

**Table 3 Inbok Lee Cases Study Result of Redundancy**

| Case No. | Structure | | | Test Period | | PFD Value | SIL Value |
|---|---|---|---|---|---|---|---|
| | Sensor (PT) | PLC | Final Element (Sol v/v, XV) | Full Stroke Test (yr) | Partial Stroke Test | | |
| 1 | 1 out of 1 (1oo1) | 1 | Sol v/v for XV : 1oo1 XV : 1oo1 | 3 | – | 4.38E–02 | SIL 1 |
| 2 | 2oo3 | 1 | Sol v/v for XV : 1oo1 XV : 1oo1 | 3 | – | 4.00E–02 | SIL 1 |
| 3 | 2oo3 | 1 | Sol v/v for each XV : 1oo1 XV : 1oo2 | 3 | – | 2.30E–03 | SIL 2 |

**Table 4 Results of Diverse Testing Period**

| Case No. | Structure: Sensor (PT) | PLC | Final Element (SOL v/v, XV) | Test Period: Full Stroke Test (yr) | Partial Stroke Test (months) | PFD Value | SIL Value |
|---|---|---|---|---|---|---|---|
| 4 | 2oo3 | 1 | Sol v/v for each XV : 1oo1 XV : 1oo2 | 3 | 6 | 1.03E–03 | SIL 2 |
| 5 | 2oo3 | 1 | Sol v/v for each XV : 1oo1 XV : 1oo2 | 3 | 3 | 9.35E–04 | SIL 3 |
| 6 | 2oo3 | 1 | Sol v/v for each XV : 1oo1 XV : 1oo2 | 3 | 2 | 9.02E–04 | SIL 3 |

## 2.8 OLGA Dynamic Multiphase Flow Simulator

OLGA dynamic multiphase flow simulator models the transient flow behavior for the entire production system from reservoir pores to the processing facilities. It aids in simulating the operational changes, such as shutdowns and startups which are inherently transient. Dynamic simulation is an essential use for onshore and offshore to examine transient behaviors in flowlines and wellbores. Since 1984, OLGA has been improved continuously due to the experimental database from the large-scale two-phase flow laboratory at SINTEF and numerical testing at IFE and in the oil companies involved.

# CHAPTER 3

# MODELLING BASES AND TUNING

The modeling part objective is to conduct a transient hydraulic simulation to predict pressure build-up time at the shut-in condition for 21 wells. The models include well model, surface piping until Pad Limit Valve (PLV) and PVT data. The well models were calibrated against field measurements to match the actual reservoir pressure, productivity index (PI), flowing wellhead pressure (FWHP), shut-in wellhead pressure (SIWHP) and flow rates. The bases to construct the 21 models are discussed below. The transient simulation analysis was conducted using OLGA V-2015 software.

## 3. 1 WELLBORE COMPONENTS

Wellbore cross-section plots for downhole equipment were provided to construct the subsurface pipes for each well which include casing and completion profiles. The data contains equipment’s total depth, diameter, and piping grades. Table 5 summarizes the tubing and last casing sizes for all wells:

**Table 5 Tubing and Casing Sizes and Lengths**

| Well | Last Casing ID (in) | Last Casing MD (ft) | Tubing ID (in) | Tubing MD (ft) |
|---|---|---|---|---|
| **A-547** | 6.276 | 7410 | 3.958 | 6504 |
| **A-430** | 4.15 | 9770 | 3.958 | 4540 |
| **A-449** | 4.15 | 6680 | 3.958 | 6447 |
| **A-485** | 6.276 | 6716 | 3.958 | 6510 |

| | | | | |
|---|---|---|---|---|
| **A-261** | 4.15 | 8557 | 3.958 | 5307 |
| **A-487** | 6.276 | 6645 | 2.992 and 3.958 | 6463 |
| **A-497** | 6.276 | 6821 | 3.958 | 6600 |
| **A-488** | 6.276 | 6600 | 3.958 | 6337 |
| **A-3001** | 6.276 | 6513 | 2.992 and 3.958 | 6084 |
| **A-145** | 6.276 | 7022 | 3.958 | 5522 |
| **A-322** | 6.276 | 6839 | 3.958 | 5513 |
| **A-324** | 6.276 | 6514 | 2.992 and 3.958 | 6084 |
| **A-512** | 6.276 | 6454 | 2.992 and 3.958 | 6224 |
| **A-543** | 6.276 | 7620 | 3.958 | 7445 |
| **A-557** | 6.276 | 6499 | 3.958 | 6429 |
| **A-560** | 6.276 | 6430 | 3.958 | 6339 |
| **B-108** | 4.15 | 8110 | 3.958 | 5800 |
| **B-131** | 4.15 | 12063 | 2.992 and 3.958 | 5882 |
| **B-322** | 4.15 | 8327 | 3.958 | 5878 |
| **B-9** | 6.276 | 6619 | 2.992 | 5383 |
| **B-251** | 4.15 | 6778 | 3.958 | 5365 |

## 3. 2 PIPELINE PROFILE

The surface piping was modelled until Pad Limit Valve (PLV), which represent the worst-case scenario for pressure build-up if suddenly closed. The model will capture the pressure build-up behavior form the bottomhole until the PLV as described in Figure 4. All wells have the same actual surface piping profiles, which were used across the 21 models. The dimensions of the surface components are provided in Table 6.

**Table 6 Surface Piping Components**

| | Length (ft) | Inner Diameter (in) |
|---|---|---|
| **Pipeline From Wellhead to Choke Valve** | 35 | 7.5 |
| **Pipeline From Choke Valve to PLV** | 35 | 7.5 |
| **PLV Size** | - | 8 |
| **Choke Valve Size** | - | 4 |

## 3. 3 PVT DATA

OLGA simulator requires Black Oil fluid file interface, i.e. PVT tables, in order to perform the transient simulation analysis. There are nine (9) downhole PVT samples available from the three fields, which were used to generate the PVT Black Oil tables for the 21 wells. The PVT samples were assigned to the 21 wells based on distance bases. The furthest distance between a well and an available PVT sample was 2 km. Laboratory reservoir fluid studies are available for the nine PVT samples, which include differential gas liberation tests. PVTsim Nova 3 software was used to generate the Black Oil tables. The assigned EOS was Peng-Robinson and was tuned with the differential gas liberation tests to match the bubble point pressure. The PVT compositions as measured in the lab are provided in Table 7.

**Table 7 Reservoir Fluid Compositions**

| | Well-1 | Well-2 | Well-3 | Well-4 | Well-5 | Well-6 | Well-7 | Well-8 | Well-9 |
|---|---|---|---|---|---|---|---|---|---|
| **N2 (mol %)** | 0.27 | 0.16 | 0.10 | 0.00 | 0.12 | 0.16 | 1.13 | 0.40 | 0.19 |

| | | | | | | | | | |
|---|---|---|---|---|---|---|---|---|---|
| **CO2 (mol %)** | 5.64 | 6.00 | 6.50 | 6.04 | 5.44 | 5.49 | 5.12 | 5.16 | 5.45 |
| **H2S (mol %)** | 1.40 | 2.40 | 2.31 | 1.52 | 1.43 | 1.43 | 0.27 | 1.63 | 1.57 |
| **C1 (mol %)** | 25.31 | 22.93 | 24.21 | 25.33 | 24.06 | 24.06 | 25.16 | 22.91 | 24.30 |
| **C2 (mol %)** | 10.67 | 9.71 | 10.21 | 9.42 | 9.98 | 9.94 | 9.27 | 9.28 | 9.83 |
| **C3 (mol %)** | 8.25 | 7.48 | 7.78 | 7.09 | 7.88 | 7.70 | 7.27 | 7.23 | 7.59 |
| **iC4 (mol %)** | 0.76 | 0.95 | 0.94 | 0.73 | 0.99 | 0.98 | 1.01 | 1.02 | 0.97 |
| **nC4 (mol %)** | 3.02 | 3.84 | 3.79 | 4.19 | 3.91 | 3.88 | 3.82 | 4.31 | 3.85 |
| **iC5 (mol %)** | 1.16 | 1.38 | 1.24 | 3.92 | 1.30 | 1.32 | 1.97 | 1.65 | 1.30 |
| **nC5 (mol %)** | 1.55 | 2.57 | 2.32 | - | 2.33 | 2.37 | 2.31 | 2.99 | 2.37 |
| **C6 (mol %)** | 3.16 | 3.58 | 2.91 | 2.52 | 3.31 | 3.53 | 2.95 | 3.69 | 3.30 |
| **C7 or C7+ (mol %)** | 38.81 | 3.47 | 37.69 | 39.24 | 39.25 | 39.14 | 3.46 | 3.54 | 39.28 |
| **C8 (mol %)** | - | 3.47 | - | - | - | - | 3.37 | 3.51 | - |
| **C9 (mol %)** | - | 2.81 | - | - | - | - | 3.51 | 3.05 | - |
| **C10+ (mol %)** | - | 29.25 | - | - | - | - | 29.38 | 29.63 | - |
| **C7+ or C10+ Density (gm/cc)** | 0.8751 | 0.8959 | 0.8712 | 0.8756 | 0.8751 | 0.8768 | 0.8931 | 0.9145 | 0.8753 |
| **C7+ or C10+ API** | 30.0 | 26.3 | 30.9 | 30.1 | 30.0 | 29.7 | 26.8 | 23.1 | 30.0 |
| **C7+ or C10+ MW** | 246 | 291 | 247 | 259 | 242 | 246 | 283 | 288 | 246 |

## 3. 4 FIELDS MEASUREMENTS

Flow rate tests data are available and were used to match and tune the model results. The rate tests data include oil rate, water cut, GOR, FWHP upstream choke valve, FWHT, and SIWHP. In addition to the rate tests parameters, the latest reservoir pressures values near each well are provided which were measured by wireline surveys. Table 8 summarizes the latest field measurements for the targeted wells.

**Table 8 Rate Tests Field Measurements for 21 Wells**

| Wells | Reservoir Pressure (psig) | Latest SIWHP (psig) | Oil Rate (BOD) | Water Cut (%) | GOR (scf/bbl) | FWHP (psig) | FWHT (F) | PI (bpd/psi) |
|---|---|---|---|---|---|---|---|---|
| **A-547** | 3847 | 1500 | 2777 | 0.5 | 513 | 1000 | 175 | 8.0 |
| **A-430** | 3563 | 1280 | 3401 | 0.0 | 587 | 1150 | 175 | 13.0 |
| **A-449** | 3787 | 1210 | 888 | 71.8 | 700 | 1150 | 175 | 16.0 |
| **A-485** | 3924 | 1260 | 1809 | 62.7 | 668 | 780 | 180 | 8.0 |
| **A-261** | 3557 | 1270 | 2648 | 3.7 | 563 | 820 | 180 | 9.0 |
| **A-487** | 3800 | 1280 | 2700 | 48.4 | 568 | 880 | 180 | 15.0 |
| **A-497** | 3726 | 1340 | 3427 | 45.1 | 545 | 1040 | 185 | 19.0 |
| **A-488** | 3544 | 1220 | 4764 | 8.3 | 621 | 780 | 180 | 9.0 |
| **A-3001** | 3554 | 1400 | 4281 | 1.0 | 574 | 760 | 160 | 10.0 |
| **A-145** | 3915 | 1460 | 2638 | 18.3 | 584 | 1180 | 180 | 11.0 |
| **A-322** | 3832 | 1240 | 2468 | 38.8 | 602 | 1160 | 175 | 23.0 |
| **A-324** | 3644 | 1380 | 4096 | 0.7 | 680 | 1280 | 180 | 37.0 |
| **A-512** | 3805 | 1400 | 2728 | 27.3 | 558 | 1340 | 180 | 39.0 |
| **A-543** | 3656 | 1460 | 6059 | 7.5 | 600 | 1300 | 180 | 32.0 |
| **A-557** | 3550 | 1280 | 2912 | 18.1 | 622 | 800 | 170 | 5.0 |
| **A-560** | 3656 | 1340 | 4088 | 22.3 | 606 | 900 | 175 | 9.0 |
| **B-108** | 3868 | 1200 | 1190 | 39.0 | 530 | 1070 | 170 | 5.0 |
| **B-131** | 3788 | 1370 | 1964 | 4.4 | 539 | 1320 | 170 | 20.0 |
| **B-322** | 3904 | 1500 | 1976 | 10.6 | 569 | 1420 | 165 | 17.0 |
| **B-9** | 3911 | 1415 | 1497 | 51.8 | 610 | 1200 | 170 | 20.0 |
| **B-251** | 3884 | 1350 | 1553 | 43.0 | 628 | 920 | 165 | 7.0 |

## 3. 5 MODEL INITIATION

There are certain parameters that were used as boundary conditions to initiate the transient hydraulic simulation for each well. The pressure boundary conditions were the reservoir pressure and the flowing wellhead pressure. The pressure boundary conditions will aid the model to predict the flow rates at stable conditions and at different operational conditions, for example, valve closure. Other boundary conditions are the reservoir temperature and the flowing wellhead temperature. The temperature boundary conditions will assist the model to estimate the heat transfer coefficients within the wellbore.

To calculate the stabilized liquid rate, the model was initiated to flow through the wellbore at time 0 seconds and continue flowing for 5 hrs (18,000 sec) where the fluid flow rate are observed to be stabilized. Then, a shutdown condition to the PLV is simulated at time 18,000 sec (closure time 5 sec) where the flow rate across the PLV turned to zero and we start monitoring the pressure build-up behavior upstream the PLV. The model was allowed to simulate the pressure build up for 43 hrs (until 172800 sec) where the pressure is stabilized and can be compared to the field SIWHP. Figure 4 shows a schematic of the wellbore and surface facilities components, and an actual OLGA model interface for one well.

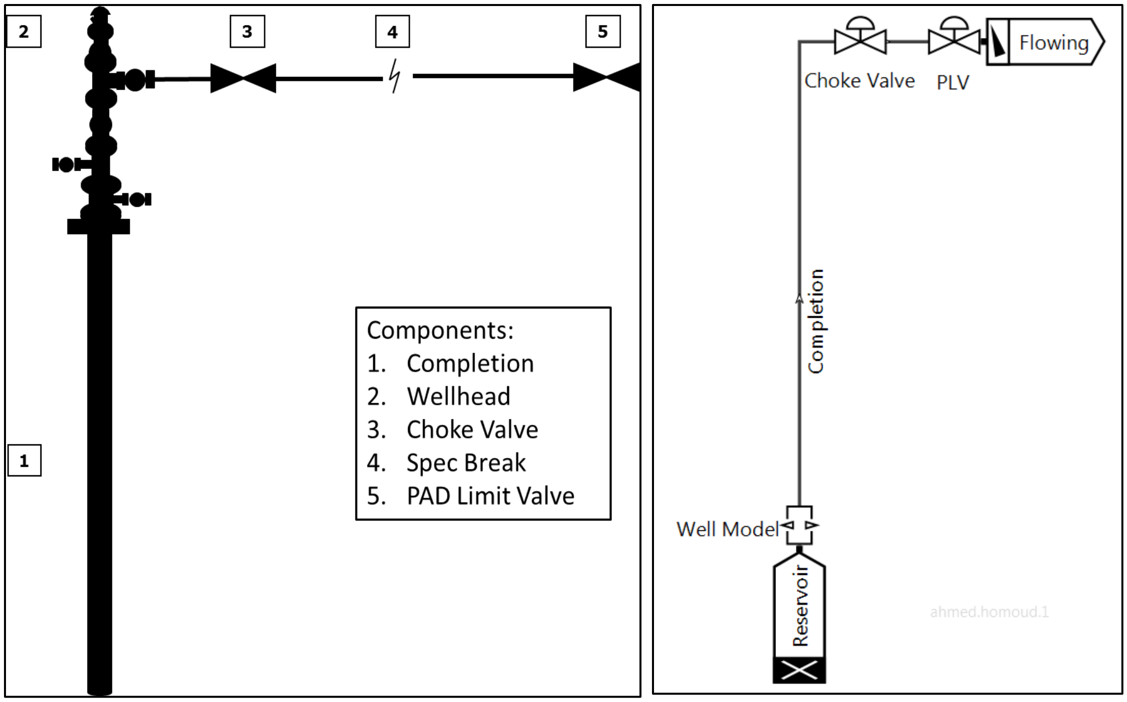


**Figure 4 Schematic of the Wellbore and Surface Facilities Components**

## 3. 6 MODEL TUNING

This section discusses the methodology to tune the PVT model and the transient hydraulic simulation model with the lab and fields data.

### 3.6.1 PVT MODEL TUNING

As discussed earlier in section 3.3, the nine (9) PVT samples data include differential gas liberation tests were available. The liberation tests data were used to tune the PVT model and to match the bubble point pressure measured in the lab. The assigned EOS was Peng-Robinson and tuning it with the lab data will improve the accuracy of the generated PVT fluid properties.  Table 9 shows the bubble point pressure data before and after tuning.

**Table 9 Bubble Point Pressure Tuning**

| PVT Samples | Lab Pb (psia) | Modelled Pb before Tuning (psia) | Modelled Pb after Tuning (psia) | Error before and after Tuning (%) |
|---|---|---|---|---|
| **1** | 1955 | 1956 | 1956 | 0.1% - 0.1% |
| **2** | 1920 | 1763 | 1910 | 8.2% - 0.5% |
| **3** | 1926 | 1885 | 1906 | 2.1% - 1.0% |
| **4** | 1924 | 1915 | 1915 | 0.5% - 0.5% |
| **5** | 1920 | 1800 | 1914 | 6.3% - 0.3% |
| **6** | 1960 | 1801 | 1935 | 8.2% - 1.3% |
| **7** | 1916 | 1850 | 1902 | 3.4% - 0.7% |
| **8** | 1950 | 1744 | 1922 | 10.6% - 1.4% |
| **9** | 1930 | 1829 | 1913 | 5.2% - 0.8% |

### 3.6.2 TRANSIENT HYDRAULIC SIMULATION MODEL TUNING

The flow rates data that were provided in section 3.4 were matched in the transient hydraulic simulation model (OLGA) to provide an accurate prediction of the pressurization behavior. Table 10 provides a comparison between the provided rate tests data and the model prediction results. In order to tune the model and to match the fields data, two parameters were slightly adjusted which are the reservoir pressures and the productivity indices (PI's). The adjustment values for reservoir pressure and PI did not exceed 87 psig and 5 bbl/psi. The adjustment values are shown in Table 11.

**Table 10 Field Data vs Model Prediction Data**

| Wells | Field Data | | Model Prediction | | Error (%) | |
|---|---|---|---|---|---|---|
| | SIWHP (psig) | Total Flow Rate (bbl/d) | SIWHP (psig) | Total Flow Rate (bbl/d) | SIWHP | Total Flow Rate |

| | | | | | | |
|---|---|---|---|---|---|---|
| **A-547** | 1500 | 2791 | 1505 | 2678 | 0.3% | 4.0% |
| **A-430** | 1280 | 3401 | 1320 | 3335 | 3.1% | 1.9% |
| **A-449** | 1210 | 3150 | 1195 | 3100 | -1.2% | 1.6% |
| **A-485** | 1260 | 4850 | 1265 | 5000 | 0.4% | -3.1% |
| **A-261** | 1270 | 2750 | 1275 | 2670 | 0.4% | 2.9% |
| **A-487** | 1280 | 5232 | 1295 | 5250 | 1.2% | -0.3% |
| **A-497** | 1340 | 6243 | 1350 | 6200 | 0.7% | 0.7% |
| **A-488** | 1220 | 5195 | 1258 | 5270 | 3.1% | -1.4% |
| **A-3001** | 1400 | 4324 | 1435 | 4260 | 2.5% | 1.5% |
| **A-145** | 1460 | 3229 | 1445 | 3150 | -1.0% | 2.4% |
| **A-322** | 1240 | 4032 | 1300 | 3875 | 4.8% | 3.9% |
| **A-324** | 1380 | 4125 | 1435 | 4250 | 4.0% | -3.0% |
| **A-512** | 1400 | 3752 | 1405 | 3625 | 0.4% | 3.4% |
| **A-543** | 1460 | 6550 | 1460 | 6540 | 0% | 0.2% |
| **A-557** | 1280 | 3555 | 1250 | 3500 | -2.3% | 1.5% |
| **A-560** | 1340 | 5261 | 1325 | 5100 | -1.1% | 3.1% |
| **B-108** | 1200 | 1950 | 1175 | 2000 | -2.1% | -2.6% |
| **B-131** | 1370 | 2054 | 1370 | 2000 | 0% | 2.6% |
| **B-322** | 1500 | 2210 | 1490 | 2180 | -0.7% | 1.4% |
| **B-9** | 1415 | 3105 | 1415 | 3030 | 0% | 2.4% |
| **B-251** | 1350 | 2725 | 1340 | 2835 | -0.7% | -4.0% |

**Table 11 Adjusted Fields Data for Model Tuning**

| Wells | Initial Field Parameters | | Adjusted Field Parameters | | Adjustment Values | |
|---|---|---|---|---|---|---|
| | PI (bpd/psi) | Pres (psig) | PI (bpd/psi) | Pres (psig) | Pres (psig) | PI (bpd/psi) |
| **A-547** | 8.0 | 3847 | 4.0 | 3760 | -87 | -4 |
| **A-430** | 13.0 | 3563 | 12.5 | 3500 | -63 | -1 |
| **A-449** | 16.0 | 3787 | 20.0 | 3875 | 88 | 4 |
| **A-485** | 8.0 | 3924 | 8.0 | 3890 | -34 | 0 |
| **A-261** | 9.0 | 3557 | 4.0 | 3510 | -47 | -5 |
| **A-487** | 15.0 | 3800 | 10.0 | 3800 | 0 | -5 |
| **A-497** | 19.0 | 3726 | 20.0 | 3795 | 69 | 1 |
| **A-488** | 9.0 | 3544 | 8.0 | 3500 | -44 | -1 |
| **A-3001** | 10.0 | 3554 | 7.2 | 3580 | 26 | -3 |
| **A-145** | 11.0 | 3915 | 9 | 3890 | -25 | -2 |
| **A-322** | 23.0 | 3832 | 21 | 3760 | -72 | -2 |
| **A-324** | 37.0 | 3644 | 40 | 3620 | -24 | 3 |
| **A-512** | 39.0 | 3805 | 35 | 3710 | -95 | -4 |
| **A-543** | 32.0 | 3656 | 30 | 3660 | 4 | -2 |
| **A-557** | 5.0 | 3550 | 5 | 3520 | -30 | 0 |
| **A-560** | 9.0 | 3656 | 8.5 | 3595 | -61 | 0 |
| **B-108** | 5.0 | 3868 | 10 | 3800 | -68 | 5 |
| **B-131** | 20.0 | 3788 | 25 | 3800 | 12 | 5 |
| **B-322** | 17.0 | 3904 | 14 | 3890 | -14 | -3 |
| **B-9** | 20.0 | 3911 | 20 | 3860 | -51 | 0 |
| **B-251** | 7.0 | 3884 | 4.8 | 3890 | 6 | -3 |

# CHAPTER 4

# RESULTS, DISCUSSIONS AND CORRELATION

This section, shows the results from the transient hydraulic simulation model. Then, the area of interest were highlighted that fits the purpose of conducting the simulation in this study. After that, sensitivity to input parameters will be highlighted to determine the most influential parameters to the results. Lastly, a correlation to predict pressure at an early shut-in time will be introduced.

## 4.1 TRANSIENT HYDRAULIC SIMULATION RESULTS

### 4.1.1 TRANSIENT SIMULATION RESULTS OF 21 WELLS

The transient hydraulic simulation results show the upstream pressure PLV vs time for 21 wells (Figure 5). From time 0 to 18,000 seconds, the pressure represents the FWHP (normal operation). Then, a shutdown condition to the PLV is simulated at time 18,000 sec (closure time 5 sec) where the flow rate across the PLV turned to zero. The pressure increases rapidly to a maximum value and then stabilizes (transient period). The model was allowed to simulate the pressure build up for 43 hrs (until 172800 sec) where the pressure is stabilized and it represents the SIWHP.

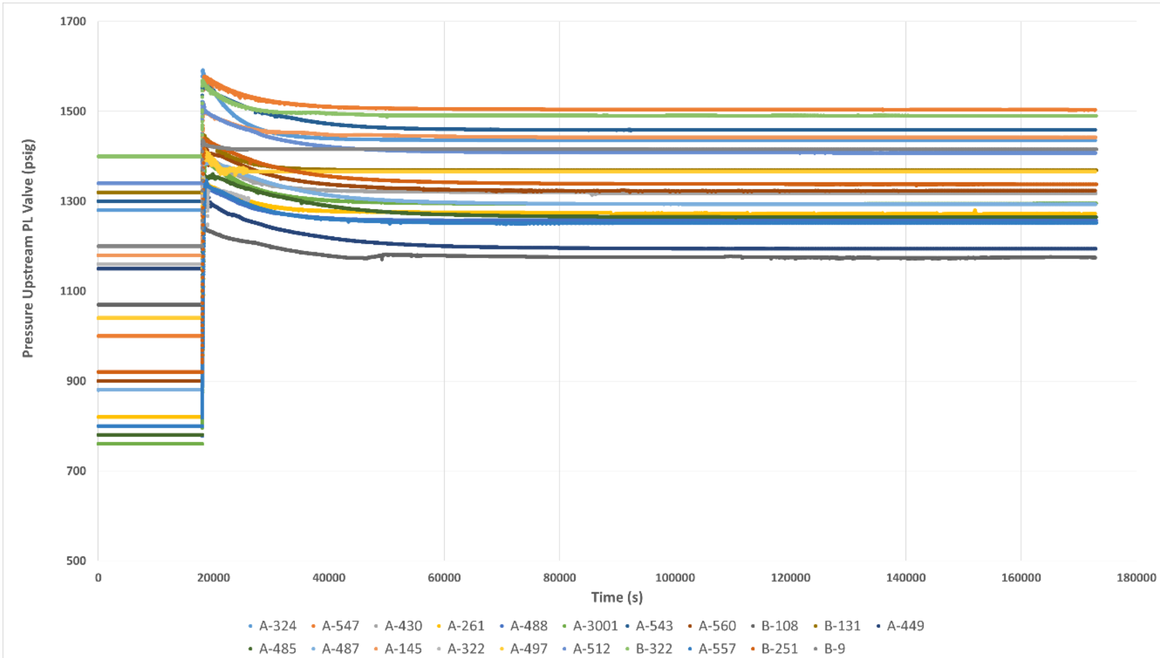


**Figure 5 Transient Simulation Results for 21 Wells**

From Figure 5, the parameters which can be identified are FWHP, SIWHP and the maximum pressure during the transient period (Pmax).

### 4.1.2 RESULTS OF INTEREST

The results presented in the previous section represent the whole simulated period which was mainly for model tuning and verification. However, the study interest is to focus on the pressure response behavior directly after PLV closure, i.e. from 18000 sec until reaching Pmax. During this period, the HIPPS valves setting pressure will be determined. Therefore, Figure 5 were zoomed into the focused area (18,000 sec to Pmax). Additionally, the time axis was reset to zero value where it represents the time at which the PLV was completely closed. Figure 6 shows the pressure behavior upstream the PLV directly after the valve was closed until it reached the maximum pressure. From Figure 6, Pmax and the time it takes each well to reach Pmax can be captured. They are tabulated in Table 12.

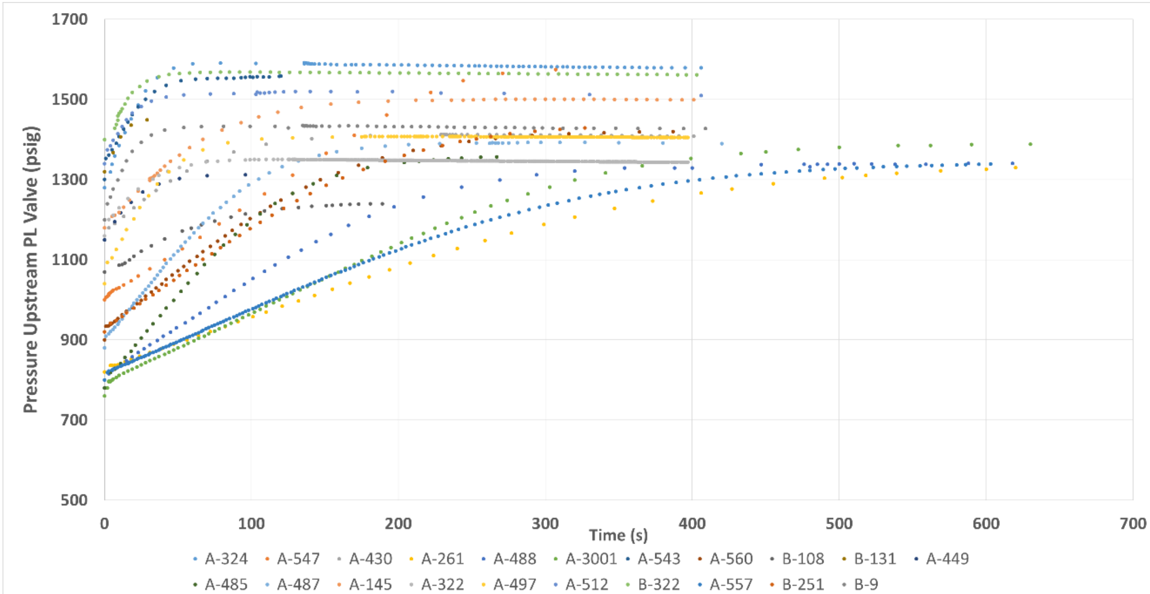


**Figure 6 Transient Simulation Results - Interest Zone**

**Table 12 Recorded Results from the Transient Simulation**

| Wells | Pmax (psig) | Time to Reach Pmax (Sec) |
|---|---|---|
| **A-547** | 1578 | 307 |
| **A-430** | 1418 | 230 |
| **A-449** | 1312 | 96 |
| **A-485** | 1356 | 267 |
| **A-261** | 1333 | 620 |
| **A-487** | 1391 | 253 |
| **A-497** | 1405 | 155 |
| **A-488** | 1340 | 618 |
| **A-3001** | 1389 | 630 |
| **A-145** | 1498 | 212 |
| **A-322** | 1312 | 102 |
| **A-324** | 1592 | 79 |

| | | |
|---|---|---|
| **A-512** | 1514 | 72 |
| **A-543** | 1556 | 120 |
| **A-557** | 1339 | 602 |
| **A-560** | 1420 | 388 |
| **B-108** | 1240 | 190 |
| **B-131** | 1449 | 29 |
| **B-322** | 1568 | 72 |
| **B-9** | 1434 | 81 |
| **B-251** | 1438 | 327 |

### 4.1.3 SENSITIVITY ON INPUT PARAMETERS

Sensitivity analysis was conducted to determine the most influential parameters to the pressure build-up behavior and build up time. The input data includes reservoir pressure, well depth (TVD and MD), PI, FWHP, oil density, water cut, wellbore volume, average fluid compressibility at flowing wellhead condition, and fluid flow rate. These parameters were analyzed against the time it takes to reach Pmax and Pmax itself. The correlation coefficient value is the method used to determine the relationship between these parameters.

Table 13 and Table 14 shows a summary of input data that were compared with the model output that were shown in Table 12.

**Table 13 Input Variables to the Transient Simulation Model**

| Wells | Reservoir Pressure (psig) | Well Depth TVD (ft) | Well Depth MD (ft) | GOR (scf/bbl) | FWHP (psig) | Fluid Compressibility (1/psi) |
|---|---|---|---|---|---|---|
| **A-547** | 3760 | 6640 | 7410 | 594 | 1000 | 1.97E-04 |
| **A-430** | 3500 | 6569 | 9770 | 632 | 1150 | 1.68E-04 |

| | | | | | | |
|---|---|---|---|---|---|---|
| **A-449** | 3875 | 6680 | 6680 | 633 | 1150 | 1.01E-04 |
| **A-485** | 3890 | 6716 | 6716 | 599 | 780 | 2.88E-04 |
| **A-261** | 3510 | 6577 | 8557 | 574 | 820 | 3.84E-04 |
| **A-487** | 3800 | 6645 | 6645 | 599 | 880 | 2.63E-04 |
| **A-497** | 3795 | 6671 | 6821 | 599 | 1040 | 1.74E-04 |
| **A-488** | 3500 | 6600 | 6600 | 599 | 780 | 4.87E-04 |
| **A-3001** | 3580 | 6765 | 9410 | 580 | 760 | 5.29E-04 |
| **A-145** | 3890 | 7022 | 7022 | 576 | 1180 | 1.42E-04 |
| **A-322** | 3890 | 6794 | 6794 | 577 | 1160 | 1.32E-04 |
| **A-324** | 3620 | 6514 | 6514 | 622 | 1280 | 1.56E-04 |
| **A-512** | 3710 | 6454 | 6454 | 622 | 1340 | 1.15E-04 |
| **A-543** | 3660 | 6500 | 7620 | 623 | 1300 | 1.50E-04 |
| **A-557** | 3520 | 6500 | 6500 | 622 | 800 | 4.14E-04 |
| **A-560** | 3595 | 6430 | 6430 | 622 | 900 | 3.35E-04 |
| **B-108** | 3800 | 7115 | 8110 | 598 | 1070 | 1.61E-04 |
| **B-131** | 3800 | 7200 | 12063 | 599 | 1320 | 6.12E-05 |
| **B-322** | 3890 | 6978 | 8377 | 577 | 1420 | 6.10E-05 |
| **B-9** | 3860 | 6619 | 6619 | 589 | 1200 | 1.05E-04 |
| **B-251** | 3890 | 6778 | 6778 | 589 | 920 | 2.26E-04 |

**Table 14 Continue Input Variables to the Transient Simulation Model**

| Wells | Oil Density (lb/ft3) | Wellbore Volume (ft3) | Water Cut (%) | Liquid Flow Rate (bbl/d) | PI (bpd/psi) |
|---|---|---|---|---|---|
| **A-547** | 53.819 | 2777 | 0.5 | 2678 | 4.0 |
| **A-430** | 53.018 | 3401 | 0.0 | 3335 | 12.5 |

| | | | | | |
|---|---|---|---|---|---|
| **A-449** | 53.018 | 1116 | 71.8 | 3100 | 20.0 |
| **A-485** | 53.619 | 1742 | 62.7 | 5000 | 8.0 |
| **A-261** | 53.799 | 2915 | 3.7 | 2670 | 4.0 |
| **A-487** | 53.619 | 2700 | 48.4 | 5250 | 10.0 |
| **A-497** | 53.617 | 3427 | 45.1 | 6200 | 20.0 |
| **A-488** | 53.629 | 4764 | 8.3 | 5270 | 8.0 |
| **A-3001** | 53.670 | 5068 | 1.0 | 4260 | 7.2 |
| **A-145** | 54.464 | 2638 | 18.3 | 3150 | 9 |
| **A-322** | 54.464 | 2685 | 38.8 | 3875 | 21 |
| **A-324** | 53.775 | 4728 | 0.7 | 4250 | 40 |
| **A-512** | 53.786 | 3397 | 27.3 | 3625 | 35 |
| **A-543** | 53.786 | 6334 | 7.5 | 6540 | 30 |
| **A-557** | 53.786 | 2912 | 18.1 | 3500 | 5 |
| **A-560** | 53.786 | 4088 | 22.3 | 5100 | 8.5 |
| **B-108** | 53.647 | 1125 | 39.0 | 2000 | 10 |
| **B-131** | 53.649 | 1964 | 4.4 | 2000 | 25 |
| **B-322** | 53.647 | 1976 | 10.6 | 2180 | 14 |
| **B-9** | 53.651 | 1540 | 51.8 | 3030 | 20 |
| **B-251** | 53.651 | 1553 | 43.0 | 2835 | 4.8 |

Table 15 shows the correlation coefficient between the input data and the model output. The analysis shows that the time it takes to reach Pmax has a strong relationship with the average fluid compressibility at flowing wellhead condition (correlation factor of 0.96). Plotting this relationship in a graph also confirms a straight-line relationship Figure 7. The relationship is as follows:

$$Time\ to\ Reach\ Pmax, sec\ [T(P_{Max})] = 1415962.31 \times Avg. Fluid\ Compressibility\ at\ FWHP\ Condition\ (\frac{1}{psi}) - 53.822$$

On the other hand, Pmax was not dependent on a single input parameter. The correlation factors were inconclusive.

**Table 15 Correlation Coefficient between the Input Data and Model Output**

| **Input Data** | **Correlation Coefficient with Time to Reach Pmax** | **Correlation Coefficient with Pmax** |
|---|---|---|
| Reservoir Pressure (psi) | -0.64 | 0.11 |
| Well Depth TVD (ft) | -0.29 | -0.14 |
| Well Depth MD (ft) | -0.04 | 0.02 |
| GOR (scf/bbl) | -0.20 | 0.15 |
| FWHP (psig) | -0.86 | 0.55 |
| **Fluid Compressibility (1/psi)** | **0.96** | -0.38 |
| Oil Density (lb/ft3) | 0.01 | 0.16 |
| Wellbore Volume (ft3) | 0.05 | -0.05 |
| Water Cut (%) | -0.30 | -0.46 |
| Liquid Flow Rate (bbl/d) | 0.13 | 0.04 |
| PI (bpd/psi) | -0.66 | 0.46 |

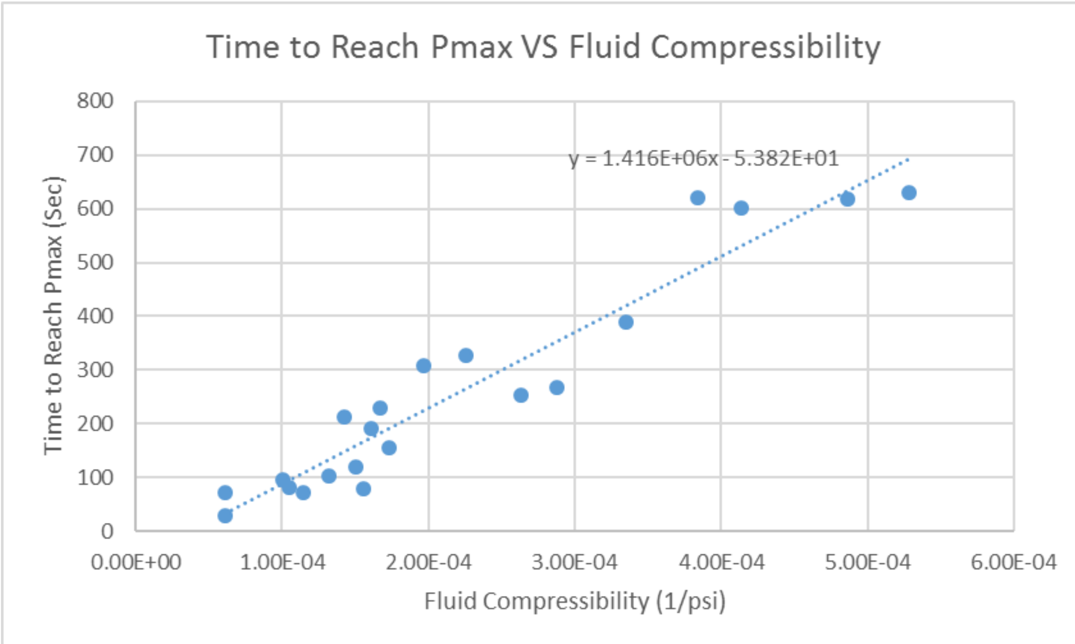


**Figure 7 Time to Reach Pmax vs Fluid Compressibility**

## 4.2 CORRELATION TO PREDICT PRESSURE AT EARLY SHUT-IN TIME

To generate a similar pressure vs time curve, we must understand how the input parameters are affecting the shape of the pressure buildup curve. To do that, each pressure buildup vs time curve of the 21 wells were analyzed individually. Looking at the shape of the curves, it is conclusive that they are a quadratic, a second-degree polynomial shape. Therefore, the idea is to obtain the a, b, and c values of the second-degree polynomial equation for each curve (curve fitting):

$$p(t) = at^2 + bt + c$$

By obtaining a, b and c values, the input parameters can be tested against them to understand how the input parameters will affect the shape of early pressure buildup curve.

Then a simplified non-linear regression approach is provided later to calculate the values of a, b, and c based on input data.

### 4.2.1 QUADRATIC CURVE FITTING

The objective of this section is to obtain the values of a, b, and c of the quadratic equation for the pressure buildup with time relation. This is done by curve fitting the 21 different curves. Figure 8 to Figure 28 show the curve fitting process. Table 16 summarizes the obtained a, b and c values.

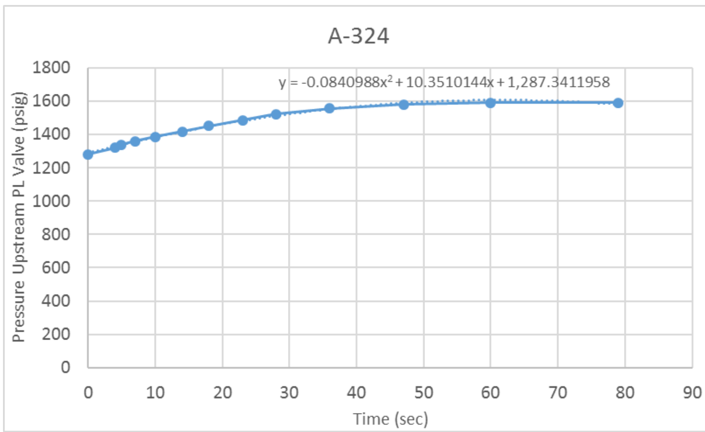


**Figure 8 Pressure Build-up Curve Fitting for Well A-324**

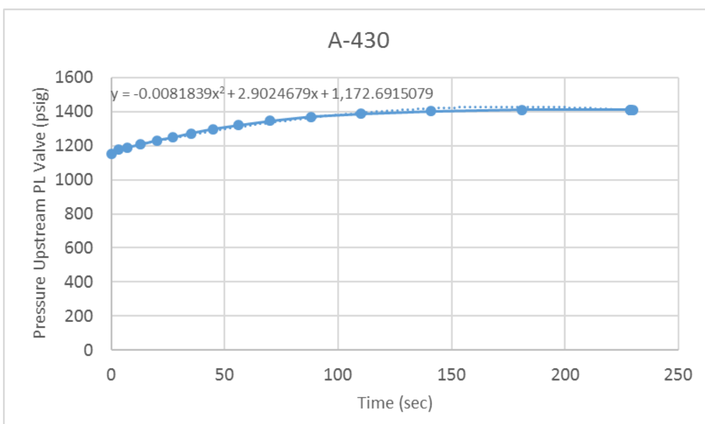


**Figure 9 Pressure Build-up Curve Fitting for Well A-430**

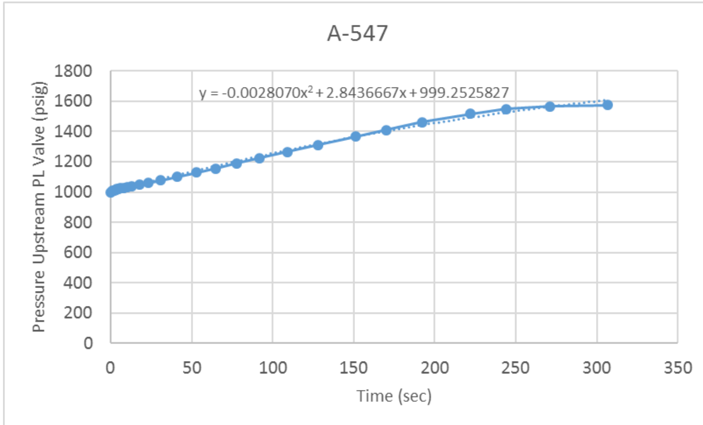


**Figure 10 Pressure Build-up Curve Fitting for Well A-547**

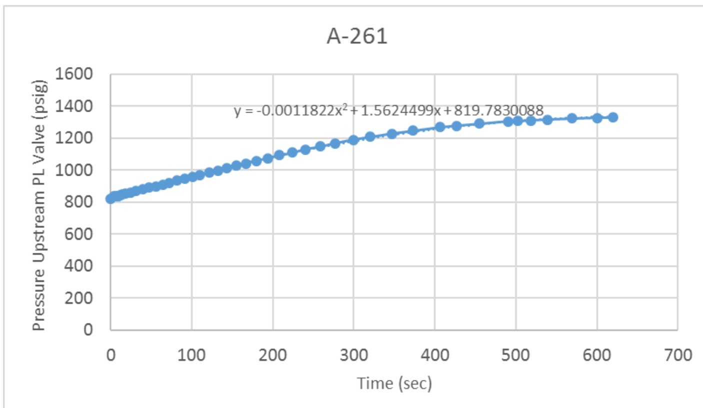


**Figure 11 Pressure Build-up Curve Fitting for Well A-261**

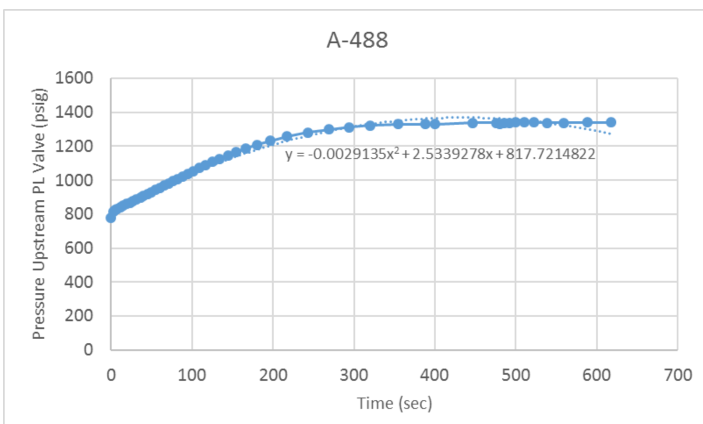


**Figure 12 Pressure Build-up Curve Fitting for Well A-488**

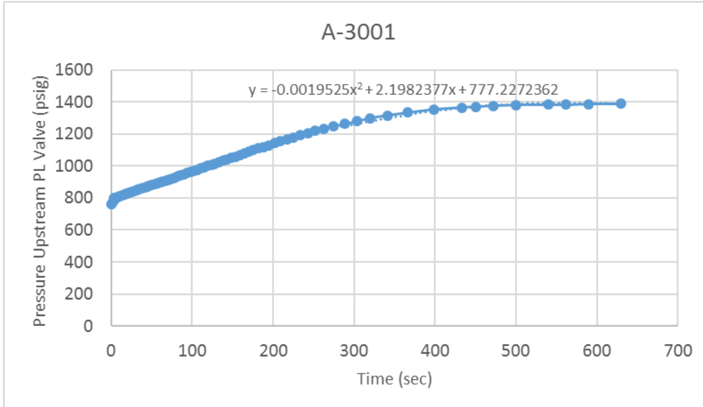


**Figure 13 Pressure Build-up Curve Fitting for Well A-3001**

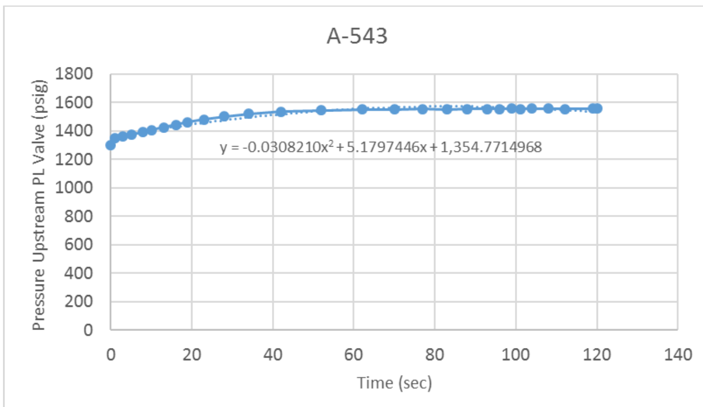


**Figure 14 Pressure Build-up Curve Fitting for Well A-543**

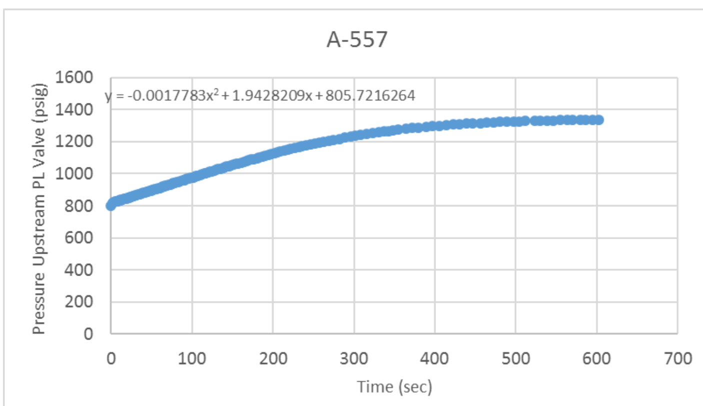


**Figure 15 Pressure Build-up Curve Fitting for Well A-557**

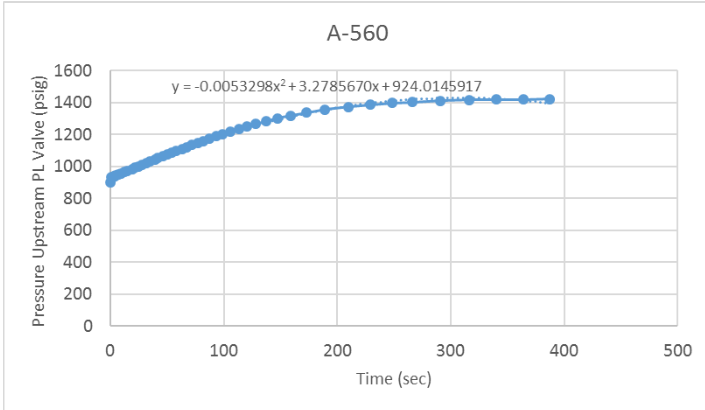


**Figure 16 Pressure Build-up Curve Fitting for Well A-560**

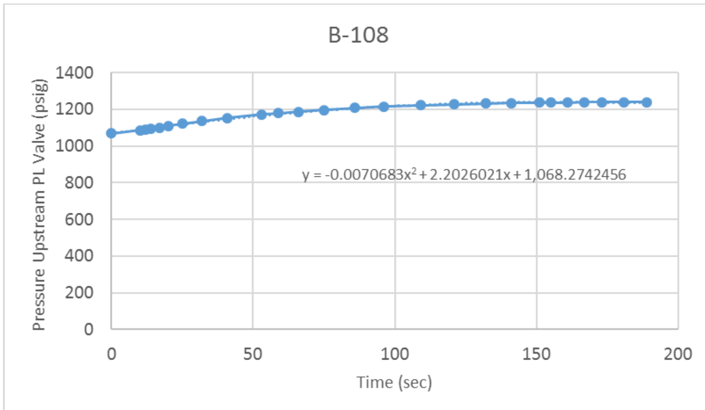


**Figure 17 Pressure Build-up Curve Fitting for Well B-108**

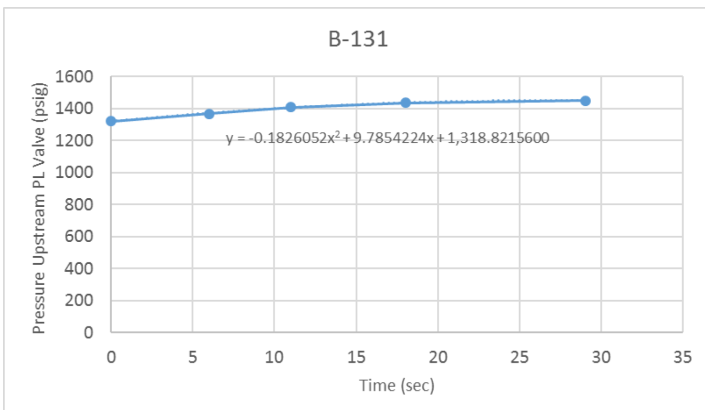


**Figure 18 Pressure Build-up Curve Fitting for Well B-131**

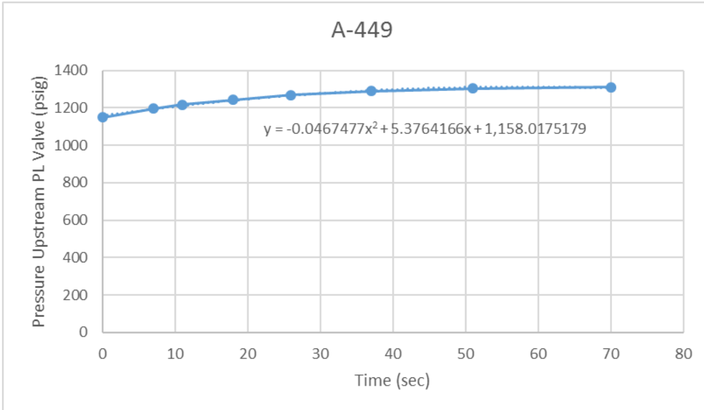


**Figure 19 Pressure Build-up Curve Fitting for Well A-449**

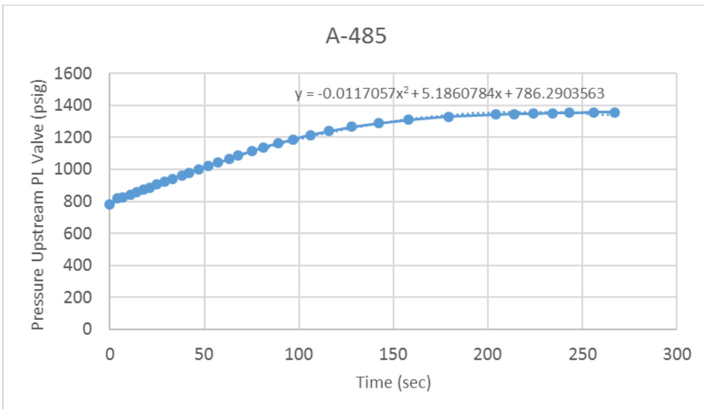


**Figure 20 Pressure Build-up Curve Fitting for Well A-485**

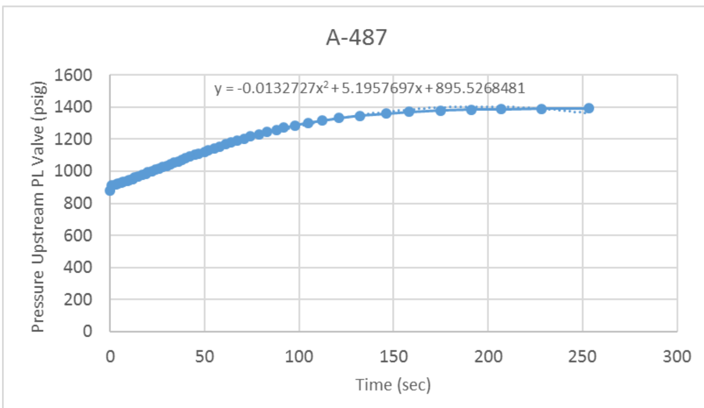


**Figure 21 Pressure Build-up Curve Fitting for Well A-487**

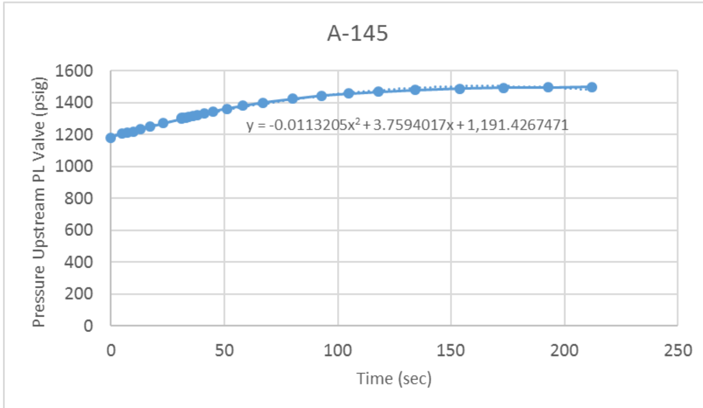


**Figure 22 Pressure Build-up Curve Fitting for Well A-145**

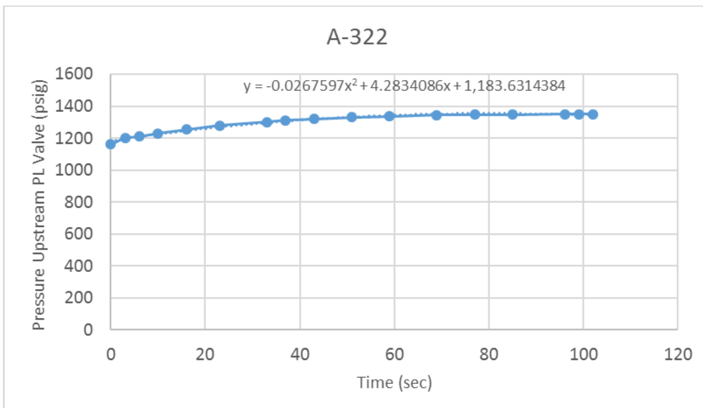


**Figure 23 Pressure Build-up Curve Fitting for Well A-322**

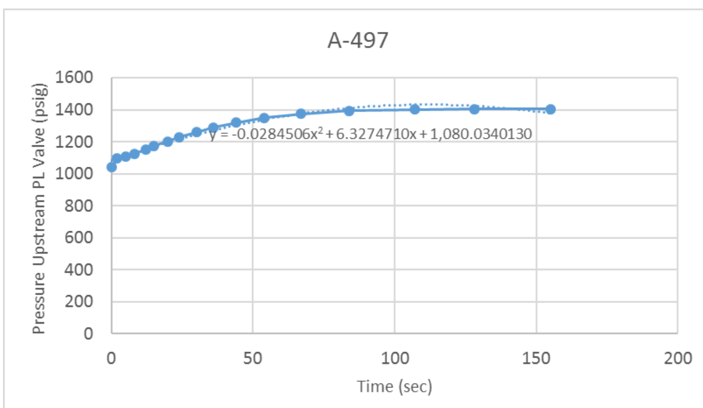


**Figure 24 Pressure Build-up Curve Fitting for Well A-497**

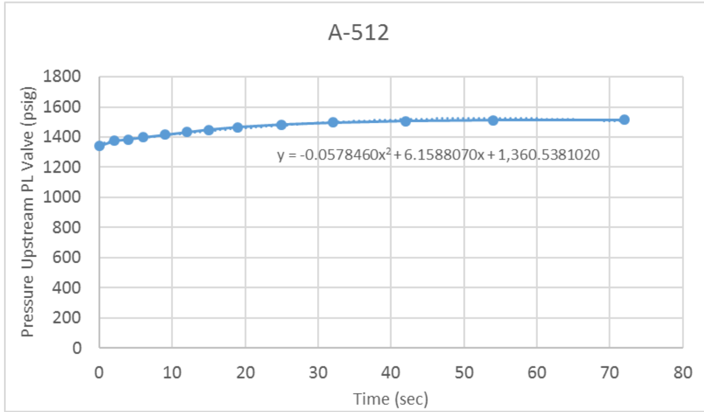


**Figure 25 Pressure Build-up Curve Fitting for Well A-512**

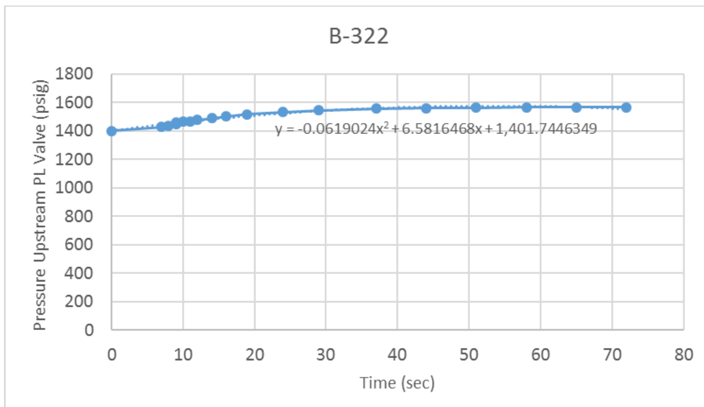


**Figure 26 Pressure Build-up Curve Fitting for Well A-322**

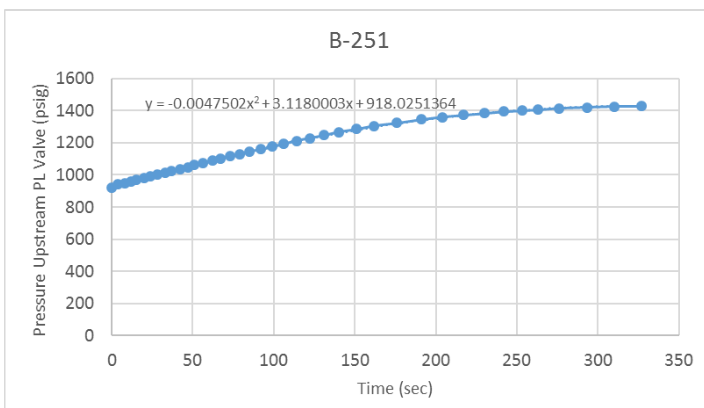


**Figure 27 Pressure Build-up Curve Fitting for Well A-251**

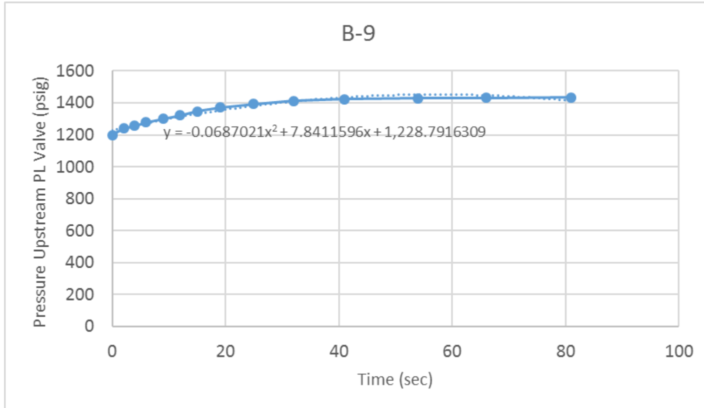


**Figure 28 Pressure Build-up Curve Fitting for Well A-322**

**Table 16 Summary of the Quadratic Equation Constants (a, b, and c)**

| Wells | a | b | c |
|---|---|---|---|
| **A-547** | -0.002807 | 2.8437 | 999.2530 |
| **A-430** | -0.008184 | 2.9025 | 1172.692 |
| **A-449** | -0.046748 | 5.3764 | 1158.018 |
| **A-485** | -0.011706 | 5.1861 | 786.2904 |
| **A-261** | -0.001182 | 1.5625 | 819.7830 |
| **A-487** | -0.013273 | 5.1958 | 895.5269 |
| **A-497** | -0.028451 | 6.3275 | 1080.034 |
| **A-488** | -0.002914 | 2.5339 | 817.7215 |
| **A-3001** | -0.001953 | 2.1982 | 777.2272 |
| **A-145** | -0.011321 | 3.7594 | 1191.427 |
| **A-322** | -0.026759 | 4.2834 | 1183.631 |
| **A-324** | -0.084099 | 10.351 | 1287.341 |
| **A-512** | -0.057846 | 6.1588 | 1360.538 |

| | | | |
|---|---|---|---|
| **A-543** | -0.030821 | 5.1797 | 1354.772 |
| **A-557** | -0.001778 | 1.9428 | 805.7216 |
| **A-560** | -0.005330 | 3.2786 | 924.0146 |
| **B-108** | -0.007068 | 2.2026 | 1068.274 |
| **B-131** | -0.182605 | 9.7854 | 1318.821 |
| **B-322** | -0.061902 | 6.5816 | 1401.745 |
| **B-9** | -0.068702 | 7.8412 | 1228.791 |
| **B-251** | -0.004750 | 3.1180 | 918.0251 |

### 4.2.2 SENSITIVITY TO QUADRATIC CURVE CONSTANTS VS INPUT DATA

Sensitivity analysis was conducted on the quadratic curve constants a, b, and c to determine how the input parameters influence the pressure build up shape. The correlation coefficient value is the method used to determine the relationship between these parameters. Table 17 shows the results of this comparison.

**Table 17 Correlation Coefficient between Input Data and a, b and c**

| Input Data | Correlation Coefficient with a | Correlation Coefficient with b | Correlation Coefficient with c |
|---|---|---|---|
| Reservoir Pressure (psi) | -0.28 | 0.39 | 0.33 |
| Well Depth TVD (ft) | -0.37 | 0.13 | 0.21 |
| **Well Depth MD (ft)** | **-0.47** | 0.10 | 0.18 |
| GOR (scf/bbl) | -0.12 | 0.18 | 0.24 |
| **FWHP (psig)** | **-0.67** | **0.67** | **1.00** |
| **Fluid Compressibility (1/psi)** | **0.58** | **-0.63** | -0.87 |

| | | | |
|---|---|---|---|
| Oil Density (lb/ft3) | 0.07 | -0.05 | 0.06 |
| Wellbore Volume (ft3) | -0.21 | -0.17 | 0.10 |
| Water Cut (%) | 0.11 | 0.09 | -0.10 |
| Liquid Flow Rate (bbl/d) | 0.28 | 0.02 | -0.20 |
| **PI (bpd/psi)** | **-0.65** | **0.79** | 0.77 |
| **Time to Reach Pmax (Sec)** | **0.63** | -0.75 | -0.86 |

The results from the sensitivity analysis revealed the following:

- c constant has a correlation coefficient of 1.00 with the FWHP, which means that c is the FWHP. This makes sense as at time equal to zero, p(t)=FWHP.
- b constant has a moderate relationship with the following input parameters: FWHP, fluid compressibility, and productivity index (PI). These input parameters will be used in the non-linear regression to estimate the value of b.
- a constant has a moderate relationship with the following parameters: FWHP, Fluid Compressibility, productivity index (PI), well measured depth and time to reach Pmax. These parameters will be used in the non-linear regression to estimate the value of a.

### 4.2.3 NON-LINEAR REGRESSION ON A AND B CONSTANTS

To estimate the values of a and b, a non-linear regression approach is performed on the dependent and independent variables. The nonlinear equations expression is as follows:

$$Y(x_1, x_2, x_3, x_4, x_5) = A(x_1)^B + C(x_2)^D + E(x_3)^F + G(x_4)^H + I(x_5)^J + K$$

The independent variables for a and b were discussed in detail in section 4.2.2 which are FWHP, Fluid Compressibility, productivity index (PI), well measured depth and time to reach Pmax. A statistical software is used to estimate the constants of the nonlinear equation (A, B, C, D, E, F, G, H, I, J, K, L, M, N, O, P, Q, and R). The results are shown below.

$$a = A(PI)^B + C(FWHP)^D + E(Fluid\ Compres.)^F + G(T(P_{Max}))^H + I(Well\ MD)^J + K$$

The constants parameters values to estimate a:

| | |
|---|---|
| A= 2.316 | G= 3.426 |
| B= 0.012 | H= 0.024 |
| C= -0.738 | I= -2.286E-42 |
| D= 0.067 | J= 9.900 |
| E= -14.397 | K= -4.972 |
| F= 0.531 | |

For b value estimates:

$$b = L(PI)^M + N(FWHP)^O + P(Fluid\ Compres.)^Q + R$$

The constants parameters values to estimate b:

| | |
|---|---|
| L= 0.065 | P= -3472.949 |
| M= 1.313 | Q= 0.001 |
| N= -280.276 | R= 3794.112 |
| O= 0.036 | |

The actual values of a and b were compared with the estimated values from the equations. They are presented in Figure 29 and Figure 30. The correlation factor for b is 0.90 and for a is 0.98.

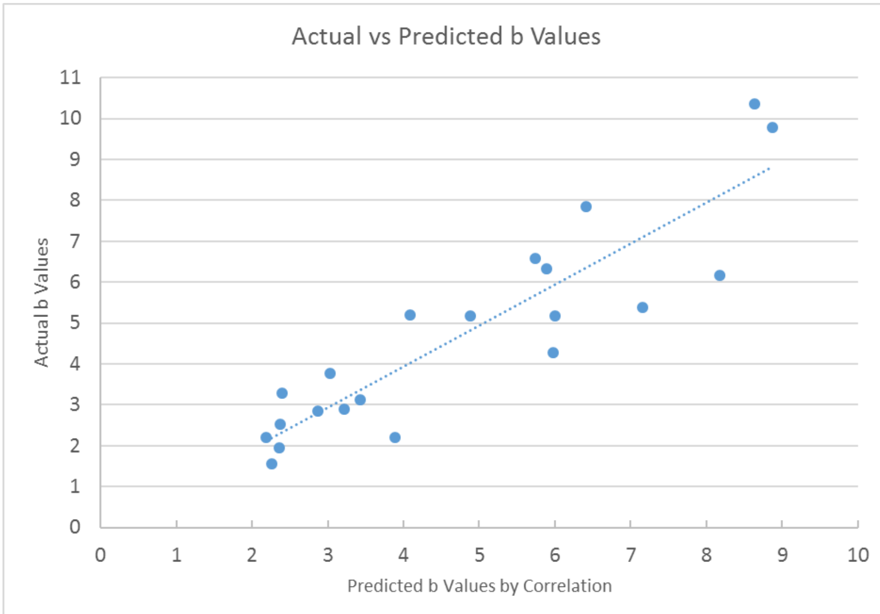


**Figure 29 Actual vs Predicted b Values**

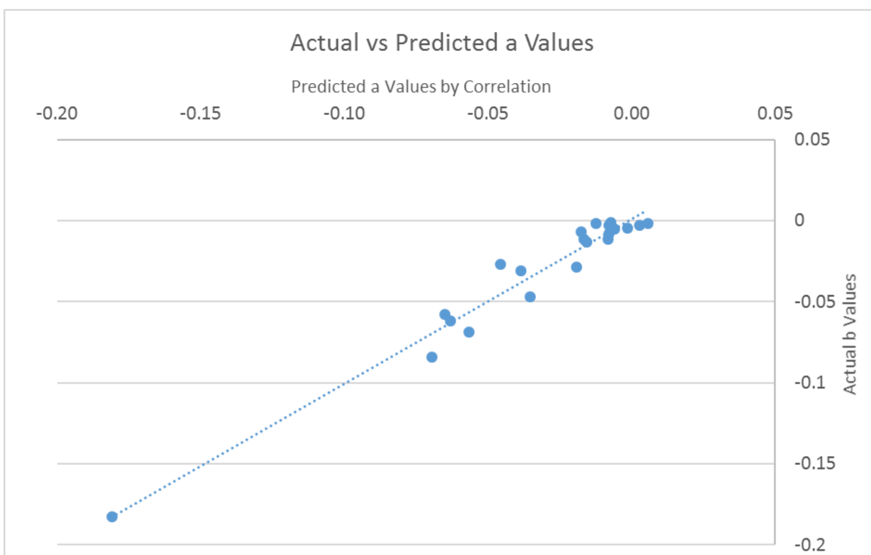


**Figure 30 Actual vs Predicted a Values**

### 4.2.4 CORRELATION PREDICTION VS ACTUAL SHUT-IN PRESSURES

As stated in section 4.2, the shape of pressure build-up curve is quadratic, a second-degree polynomial shape. From the previous section discussions, the correlation is concluded as follows:

$$P(t) = at^2 + bt + c$$

Where,

$$a = A(PI)^B + C(FWHP)^D + E(Fluid\ Compres.)^F + G(T(P_{Max}))^H + I(Well\ MD)^J + K$$

$$b = L(PI)^M + N(FWHP)^O + P(Fluid\ Compres.)^Q + R$$

$$c = FWHP$$

All constants values were presented in section 4.2.3.

The above correlation was used to regenerate the 21 early shut-in pressure vs time profiles to test the accuracy of the correlation results. The actual vs predicted by the correlation pressure values are plotted in Figure 31 to Figure 43. The standard deviation and standard error in calculating the pressure for each well are presented in Table 18.

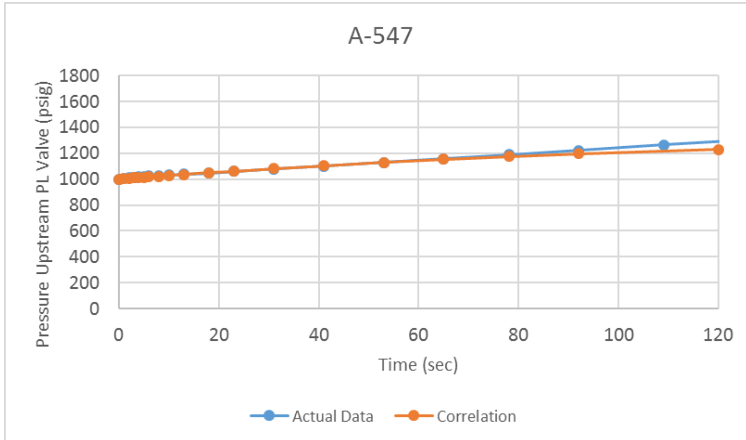


**Figure 31 Correlation Prediction vs Simulation Results for A-547**

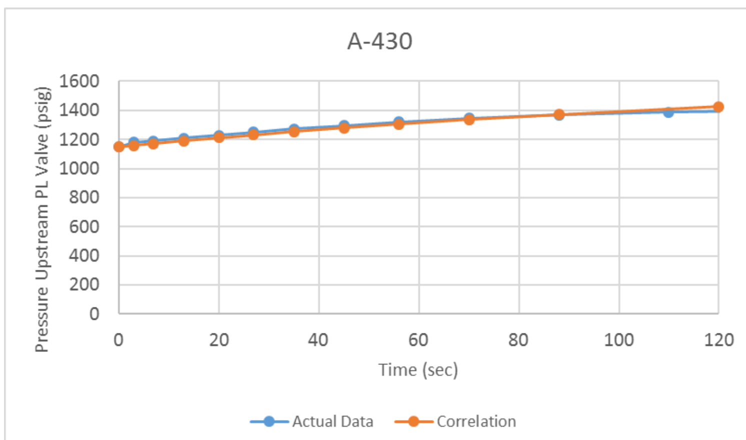


**Figure 32 Correlation Prediction vs Simulation Results for A-430**

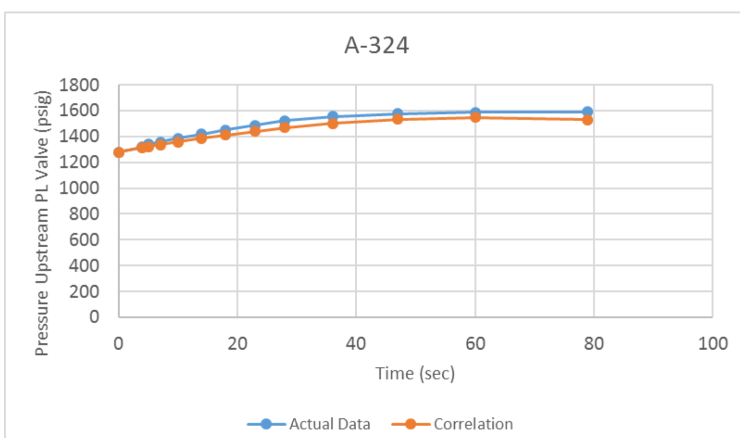


**Figure 33 Correlation Prediction vs Simulation Results for A-324**

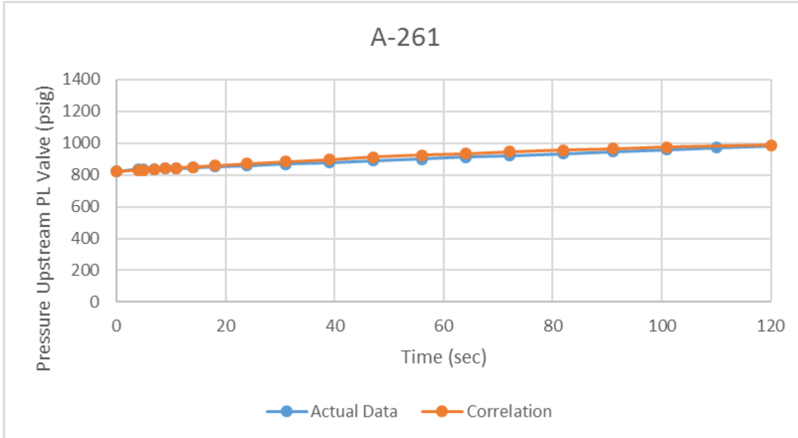


**Figure 34 Correlation Prediction vs Simulation Results for A-261**

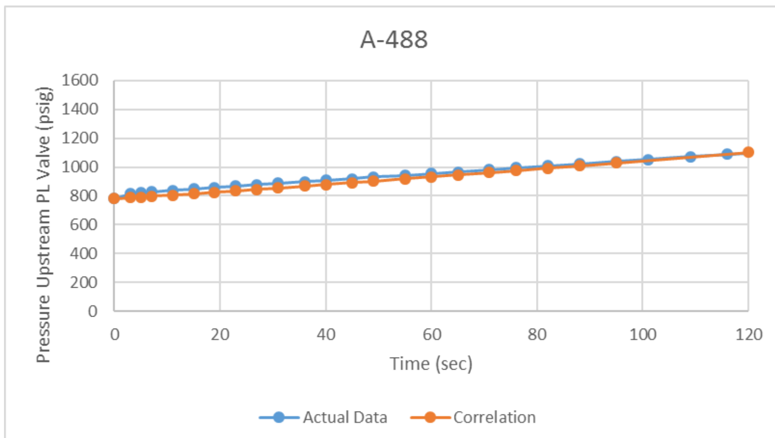


**Figure 35 Correlation Prediction vs Simulation Results for A-488**

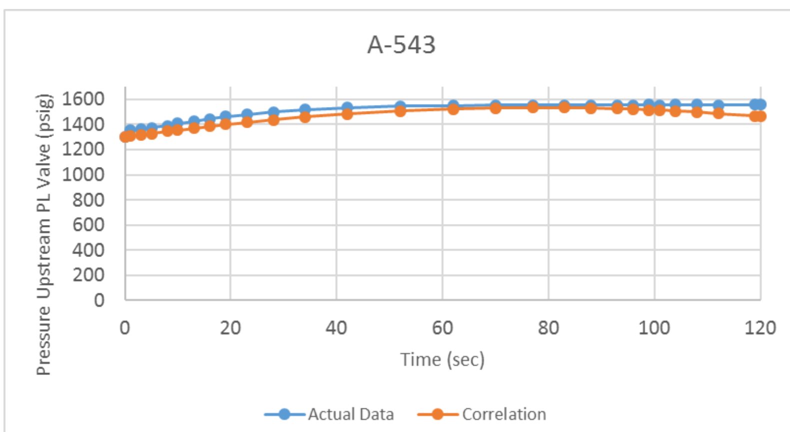


**Figure 36 Correlation Prediction vs Simulation Results for A-543**

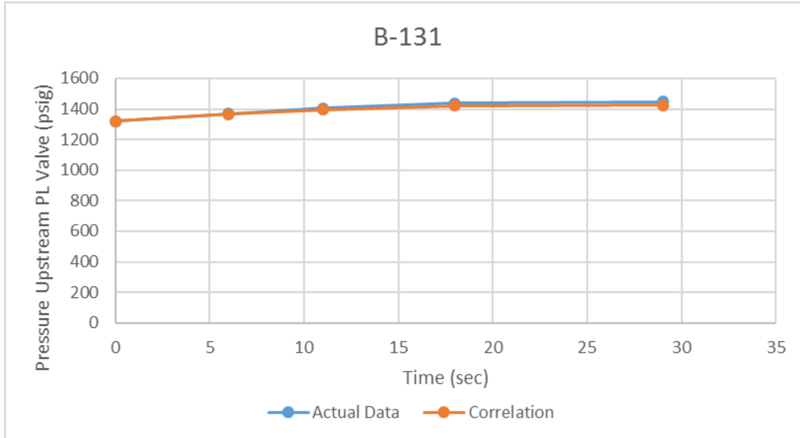


**Figure 37 Correlation Prediction vs Simulation Results for B-131**

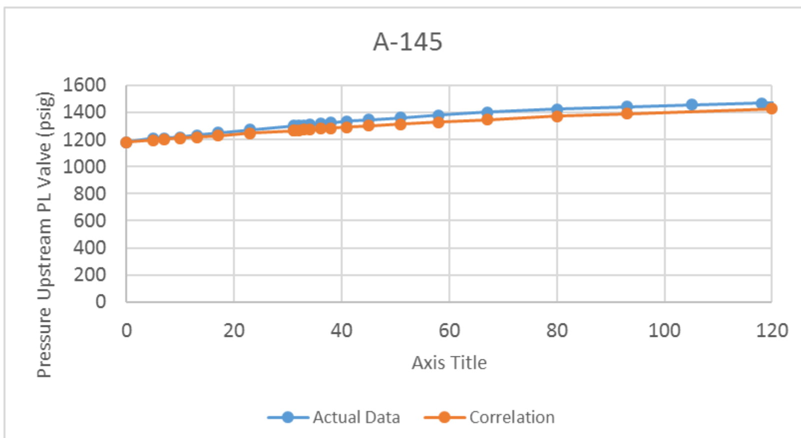


**Figure 38 Correlation Prediction vs Simulation Results for A-145**

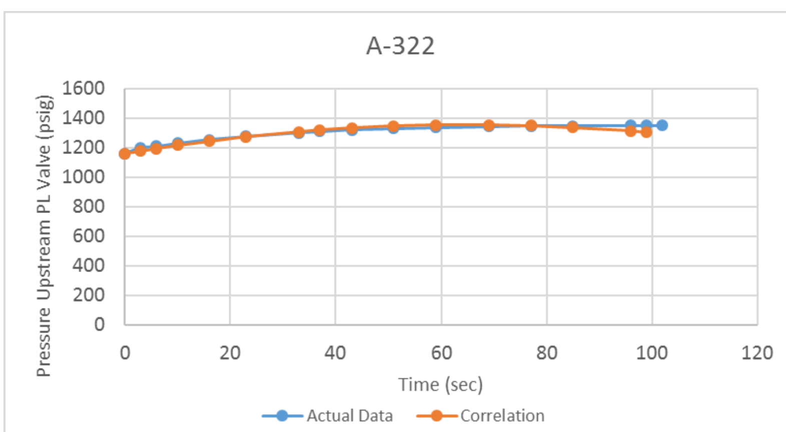


**Figure 39 Correlation Prediction vs Simulation Results for A-322**

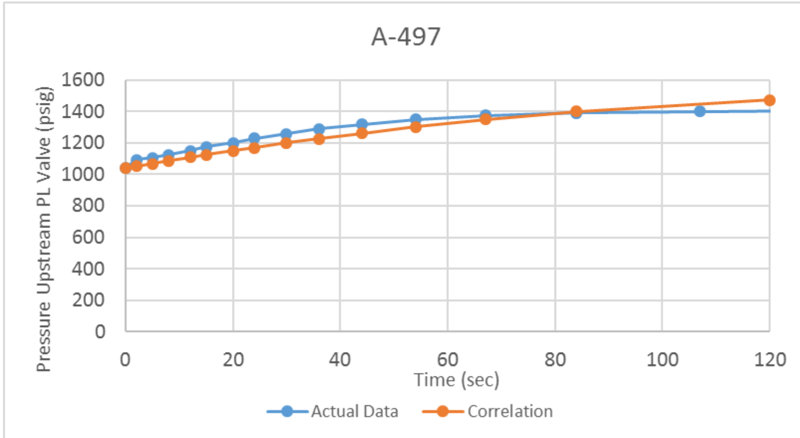


**Figure 40 Correlation Prediction vs Simulation Results for A-497**

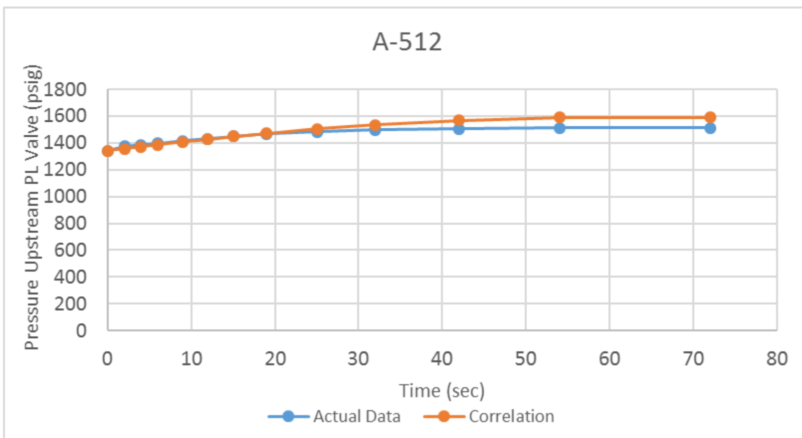


**Figure 41 Correlation Prediction vs Simulation Results for A-512**

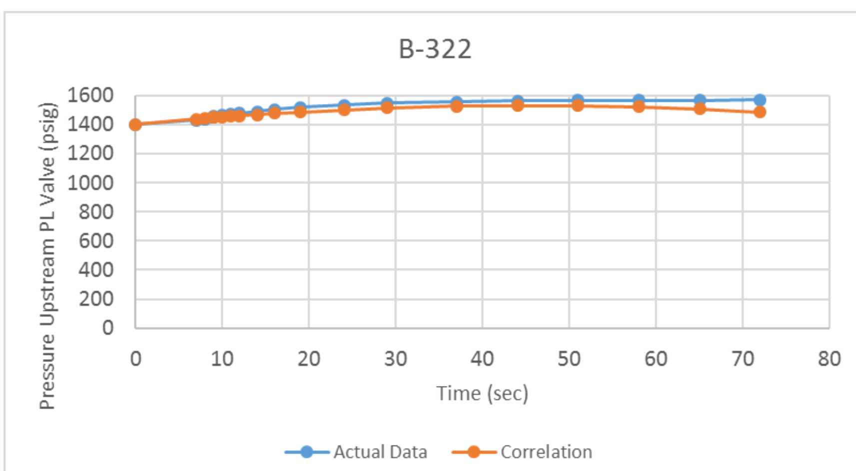


**Figure 42 Correlation Prediction vs Simulation Results for B-322**

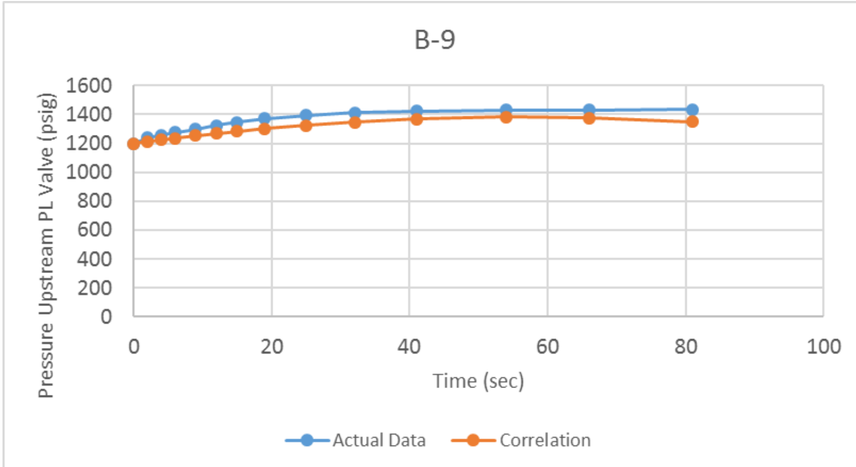


**Figure 43 Correlation Prediction vs Simulation Results for B-9**

**Table 18 Standard Deviation & Error between Correlation & Simulation Results**

| Wells | Standard Deviation | Standard Error (psig) |
|---|---|---|
| **A-547** | 63.2 | 14.5 |
| **A-430** | 70.1 | 21.1 |
| **A-449** | 99.8 | 33.3 |
| **A-485** | 97.7 | 15.3 |
| **A-261** | 46.7 | 11.0 |
| **A-487** | 97.7 | 15.3 |
| **A-497** | 110.7 | 29.6 |
| **A-488** | 61.4 | 14.1 |
| **A-3001** | 51.3 | 8.5 |
| **A-145** | 65.7 | 14.3 |
| **A-322** | 62.7 | 15.7 |
| **A-324** | 98.9 | 27.4 |
| **A-512** | 73.0 | 20.2 |

| | | |
|---|---|---|
| **A-543** | 85.4 | 18.2 |
| **A-557** | 69.7 | 9.3 |
| **A-560** | 79.0 | 14.4 |
| **B-108** | 61.9 | 16.0 |
| **B-131** | 43.5 | 19.4 |
| **B-322** | 62.7 | 15.7 |
| **B-9** | 74.0 | 19.8 |
| **B-251** | 87.5 | 19.1 |

### 4.2.5 CORRELATION VALIDATION

To validate the correlation, data from three wells that were not included in the model initiation process are being entertained. The input data are tabulated below in Table 19. The calculations to plot the pressure vs time is also shown below. Then the actual vs predicted figures are plotted in Figure 44, Figure 45 and Figure 46.

**Table 19 Fields Data for Validation**

| Wells | FWHP | Well Depth MD | Fluid Compressibility | PI |
|---|---|---|---|---|
| A-1 | 1320 | 7271 | 1.054E-04 | 31 |
| A-2 | 1200 | 7635 | 1.7245e-4 | 22 |
| A-3 | 960 | 9682 | 3.8417e-4 | 22 |

First, calculate the time it takes to reach Pmax, T(Pmax) using the equation presented in section 4.1.3:

$Time\ to\ Reach\ Pmax, sec\ [T(P_{Max})] = 95$ seconds for A1, 190 seconds for A2 and 490 seconds for A3.

Then calculate the values of a, b and c using the equations presented in section 4.2.3:

a= -0.03667 for A1, -0.00826 for A2, and 0.01640 for A3

b= 7.7399 for A1, 4.5044 for A2, and 3.5930 for A3

c= 1320 for A1, 1200 for A2, and 960 for A3.

After that, use these coefficients in the quadratic equation presented in section 4.2 to plot the early pressure build-up vs time. Figure 44, Figure 45 and Figure 46 shows the actual data vs the predicted curve by the correlation.

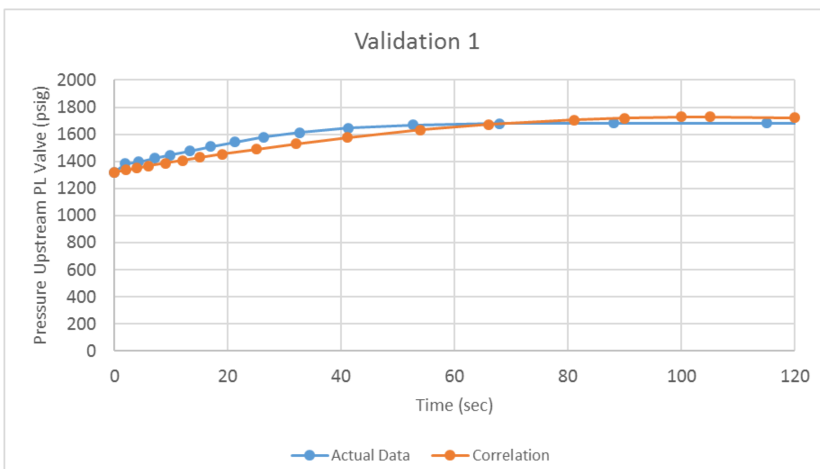


**Figure 44 Actual Data vs Predicted Data - Model Validation Well#A1**

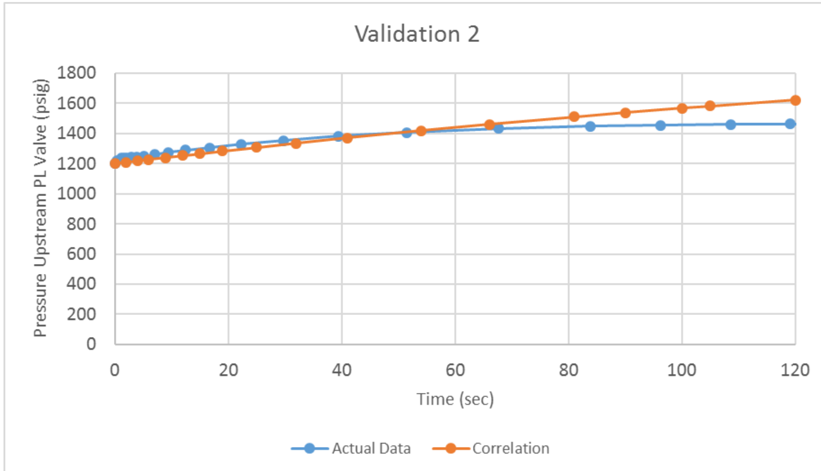

**Figure 45 Actual Data vs Predicted Data - Model Validation Well#A2**

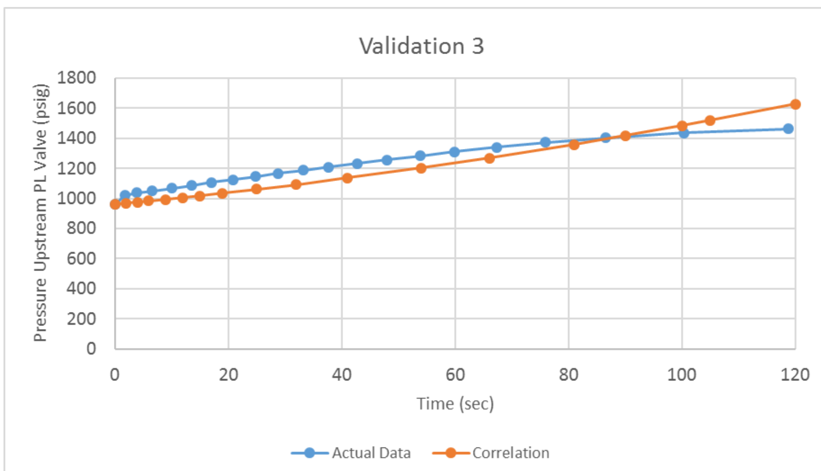

**Figure 46 Actual Data vs Predicted Data - Model Validation Well#A3**

From the previous validation charts, the correlation estimates the pressure build-up at an early shut-in time well. However, it tends to overestimate the pressure at a late time i.e. after 60 seconds. Therefore, this correlation is valid only between the time frame of 0 seconds and T(Pmax) or 60 second, which one is lower. Yet this correlation is very useful as the HIPPS response happens between the time frame of 5 to a maximum 40 seconds, depending on HIPPS valves type and manufacturer.

### 4.2.6 FIELD TEST VERIFICATION

A shut-in field test was conducted on one well (Well-21) to monitor the wellbore pressure build-up behavior with time. The test duration was 50 seconds. The recorded data are presented in Figure 47 to Figure 52. The test could not be extended further not to lose the field target production. Yet, the gathered information is enough to compare the early time pressure build-up predicted by the correlation versus actual field test. Table 20 summarizes the input data to the model, which are fields measurements for Well-21. Table 21 showed the correlation calculated parameters to generate the pressure vs time curve. Figure 53 compares the correlation output with the field test measurements.


**Figure 47 Pressure Readings at Shut-in Time = 0 sec**


**Figure 48 Pressure Readings at Shut-in Time = 10 sec**


**Figure 49 Pressure Readings at Shut-in Time = 20 sec**


**Figure 50 Pressure Readings at Shut-in Time = 30 sec**


**Figure 51 Pressure Readings at Shut-in Time = 40 sec**


**Figure 52 Pressure Readings at Shut-in Time = 50 sec**

**Table 20 Well-21 Fields Data for Validation**

| Well | FWHP | Well Depth MD | Fluid Compressibility | PI |
|---|---|---|---|---|
| 21 | 805 | 13,450 | 1.90E-04 | 28 |

**Table 21 Correlation Calculated Parameters for Well-21**

| a | b | c |
|---|---|---|
| -0.136 | 10.61 | 805 |

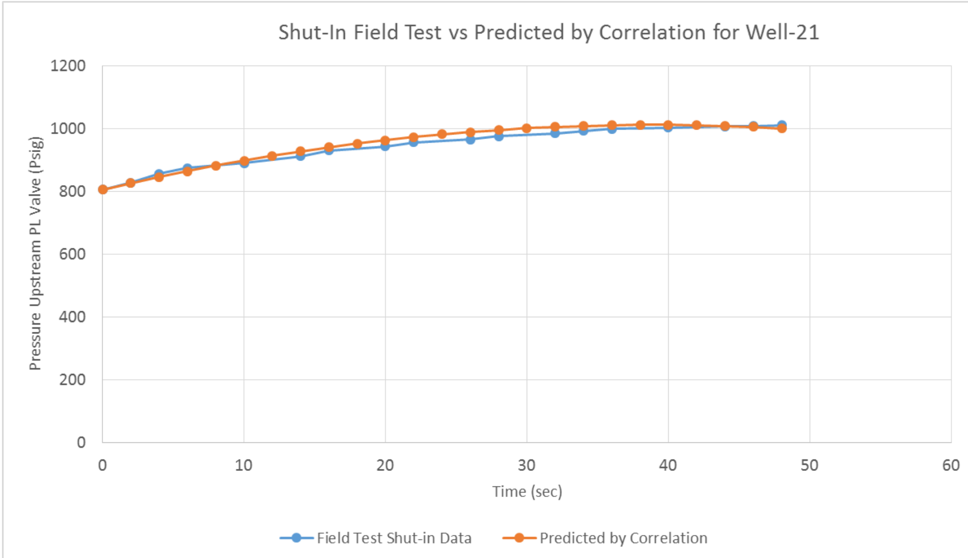


**Figure 53 Shut-in Field Test Measurements vs Correlation Prediction for Well-21**

The correlation estimated the pressure build-up behavior very well compared with the field test measurements. This validation enhanced the confidence on using the developed correlation. The statistical analysis between the correlation prediction and field measurements are shown below in Table 22.

**Table 22 Statistical Analysis for Well-21**

| | |
|---|---|
| Standard Deviation | 66.5 |
| Standard Error | 15.7 psig |

## 4.3 APPLICATIONS TO THE DEVELOPED CORRELATION

### 4.3.1 HIPPS RESPONSE TIME VERIFICATION

HIPPS valves respond to high pressure events within 5 to a maximum of 40 seconds, depending on HIPPS valves type and manufacturer. By understanding the behavior of the pressure build-up at early time under shut-in condition, engineers can decide on the type of HIPPS valves and manufacturers. To illustrate the point, a hypothetical example is given about well# B-9. Assuming the downstream pipeline rating is 1350 psig, the build-up pressure results are shown in Figure 54 along with the downstream pipeline rating. In this case, there is only 15 seconds between the valve closure until the pressure reaches the maximum allowable pressure (rupture point). This leaves a very narrow window for the HIPPS to react. There are two solutions to such case, one is to install an expensive system that will ensure reaction less than 15 seconds, and another one is to reduce the FWHP to a point where the pressure build-up window is within the HIPPS reaction time window.

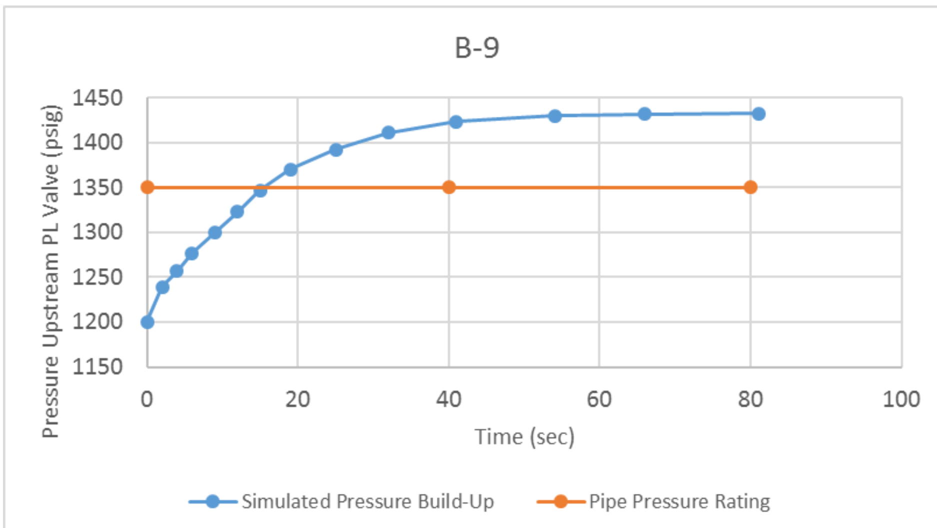


**Figure 54 Well B-9 Pressure Build-Up Profile vs Pipeline Maximum Pressure**

### 4.3.2 ACTIONS TO ENSURE SAFE OPERATIONS

As discussed in well# B-9 example in section 4.3.1, one solution to ensure safe operation is to reduce the FWHP to a point where the pressure build-up window is within the HIPPS reaction time. This scenario can be simulated by the newly developed correlation. By reducing the FWHP, the pressure build-up curve can be regenerated. The new pressure curve (Figure 55) can be compared with the old one (Figure 54) and make suitable decision based on the outcome.

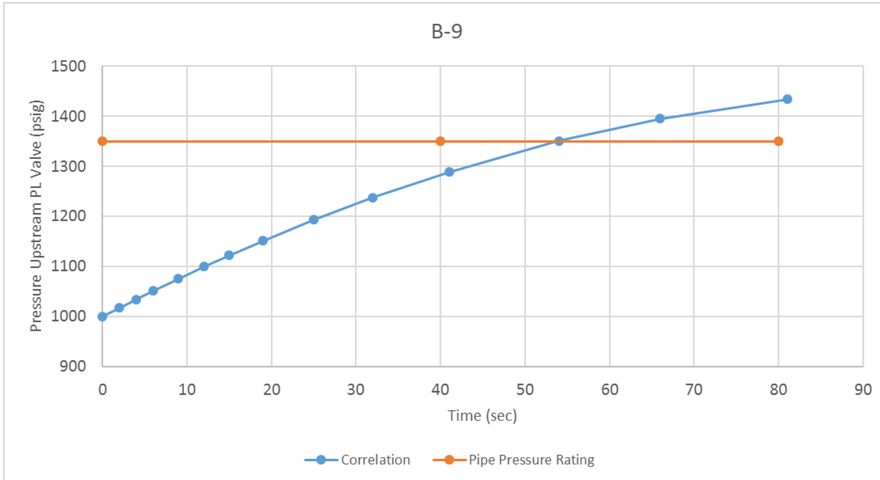


**Figure 55 Updated Pressure Build-Up Profile vs Pipeline Maximum Pressure**

# CHAPTER 5

# CONCLUSION

The work presented in this thesis showed a methodology to conduct a transient wellbore flow assurance analysis under sudden valve closure condition. It presented a tuning mechanism for the PVT and transient simulation models. It discussed curve fitting and nonlinear regression methods to understand the influence of the studied parameters on pressure buildup behavior with time.

In conclusion, a new empirical correlation was developed to estimate the early time wellbore pressure build-up under sudden PL valve closure condition. The correlation is a function of reservoir, fluid and wellbore parameters, as follows:

$$P(t) = at^2 + bt + c$$

Where,

$$a = A(PI)^B + C(FWHP)^D + E(Fluid\ Compres.)^F + G(T(P_{Max}))^H + I(Well\ MD)^J + K$$

$$b = L(PI)^M + N(FWHP)^O + P(Fluid\ Compres.)^Q + R$$

$$c = FWHP$$

The correlation has been calibrated and verified with field tests data. It showed a great match at an early shut-in time. However, it tends to overestimate the pressure at the late time, after 60 seconds. Therefore, this correlation is only valid between the time frame of 0 seconds and 60 seconds or T(Pmax), which one is lower.

Among the studied parameters, the study concluded that the most influential parameters on the pressure build-up behaviors are Fluid Compressibility, Productivity Index. FWHP, and Well Measured Depth. These parameters were considered when developing the new correlation.

The study also concluded that there is a strong relationship between the fluid compressibility at FWHP condition and the time it takes to pressurize the wellbore to maximum pressure. The higher the fluid compressibility, the longer time it takes the system to pressurize.

Lastly, field's HIPPS applications to the developed correlation were discussed including HIPPS response time verification and proper actions to ensure safe operations.

# References


[1] American Petroleum Institute (2014). API 17O Standard for Subsea High Integrity Pressure Protection System (HIPPS), Second Edition. Washington, DC: API.

[2] Aruo, R., Lund B., Onshus, T. 1995. Subsea HIPPS Design Procedure. Presented at the Offshore Technology Conference, Houston, Texas, U.S.A., 1-4 May 1995. OTC-7829-MS.

[3] Curran, C., 2006. Development and Approval of High Integrity Pressure Protection Systems (HIPPS) for Application in the Gulf of Mexico. Presented at the Subsea Controls and Data Acquisition 2006: Controlling the Future Subsea conference, 7-8 June, Neptune, France. SUT-SCADA-06-112.

[4] Curran, C., 2008. High Integrity Pressure Protection Systems (HIPPS) Development for the Gulf of Mexico: Update on Deepstar, API 17O and Industry Developments. Presented at the Offshore Technology Conference, Houston, Texas, U.S.A., 5-8 May 2008. OTC- 19703-MS.

[5] Frafjord, P., Corneliussen, S. and Adriaansen, L. 1995. The development of a Subsea High Integrity Pipeline Protection System (HIPPS). Presented at the 27th Annual OTC, Houston, Texas, U.S.A., 1-4 May 1995. OTC-7833.

[6] Gall, G., Turner, P., and Seaton, R. 2002. Reliability of Subsea Control Systems: HIPPS a case Study. Presented at the Subsea Controls and Data Acquisition Conference, Paris, France, 14 June 2002. OTC-27278-MS. SUT-SCADA-02-055.

[7] Hernandez, R., Patel, R., Attawat, T. et al. 2016. Implementation and Challenges of a SIL 3 Subsea HIPS. Presented at the Offshore Technology Conference, Houston, Texas, U.S.A., 2-5 May 2016. OTC-27278-MS.

[8] Hoseth, J., Willmann, E., and Roberts, P. 1997. Implementation Options for the Subsea High Integrity Pipeline Protection System (HIPPS) Solution. Presented at the Offshore Technology Conference, Houston, Texas, U.S.A., 5-8 May 1997. OTC-8450-MS.

[9] Hutchings, V., 2010. Is the Subsea High Integrity Pressure Protection System (HIPPS) Coming of Age?. Presented at the Subsea Controls and Data Acquisition (SCADA) Conference, 2-3 June, Newcastle, UK. SUT-SCADA-10-169.

[10] International Electro-technical Commission (2000). IEC 61508 Functional Safety of Electrical/Electronic/Programmable Electronic Safety-Related Systems.

[11] International Electro-technical Commission (2003). IEC 61511 Functional safety – Safety Instrumented Systems for the Process Industry Sector.

[12] Lee, I. and Taekeun, O., 2013. A Study of Flare Load Reduction by a Safety Instrumented System based on a High Integrity Protection System. Process Safety Progress 32 (04): 393–400. DOI 10.1002/prs.11608

[13] Minerals Management Service and Granherne Limited. 2010. Evaluation of High Integrity Pressure Protection Systems. Final report, Project Number: J5920-MMS-RT-U-007, Houston, TX 77002-7900, USA (12 Apr 2010).

[14] Moroney, M., Kvaerner, M. 1995. HIPS Design and Applications. Presented at the Offshore Europe Conference in Aberdeen, 5-8 September 1995. SPE-030394.

[15] Norwegian Oil Industry Association (2004). OLF 070 Application of IEC 61508 and IEC 61511 in the Norwegian Petroleum Industry.

[16] Patni, S. and Davalath, J. 2002. Subsea HIPPS: A Way to Develop High-Pressure Subsea Fields. Presented at the SPE Annual Technical Conference and Exhibition, Houston, Texas, U.S.A., 26-29 September 2002. SPE-89998-MS.

[17] Phillips, R. 2005. Delivering a HIPPS Safety Critical Control System. Presented at the Offshore Europe Conference, Aberdeen, United Kingdom, 6-9 September 2005. SPE-96757-MS.

[18] Politis, N., Banon, H., and Curran, C. 2013. HIPPS-Based No-Burst Design of Flowlines and Raisers. SPE Oil and Gas Facilities 2 (02): 42-50. SPE-163051-PA.

# Vitae

Name :Ahmed Abdulkarim Abdullah Homoud

Nationality :Saudi Arabia

Date of Birth :8/28/1987

Email :Ahmed.Homoud.1@aramco.com

Address :P.O. Box 13342, Dhahran 31311, Saudi Arabia

Academic Background :Bachelor of Engineering Awarded with Second Class Honors in Petroleum Engineering from The University of Adelaide, Australia.

Presented Papers :

Homoud, A., Ayub, M., and Mohammed E. 2017. Integrated Topographic Multiphase Flow Modeling in Surface Pipelines – A Case Study. Presented at the SPE Kingdom of Saudi Arabia Annual Technical Symposium and Exhibition, Dammam, Saudi Arabia, 24-27 April 2017. SPE-188117-MS.